Nature Communications

https://doi.org/10.1038/s41467-026-73123-y

Article in Press

TaMPK3 mediates synergistic damage from *Fusarium* crown rot and drought in wheat

Received: 17 July 2025

Accepted: 2 May 2026

Cite this article as: Zheng, L., Yu, T.-F., Liu, Y. *et al.* TaMPK3 mediates synergistic damage from *Fusarium* crown rot and drought in wheat. *Nat Commun* (2026). https://doi.org/10.1038/s41467-026-73123-y

Lei Zheng, Tai-Fei Yu, Ying Liu, Ze-Hao Hou, Ji-Tong Wei, Jia-Min Hao, Xing-Yu Liu, Xin-Rui Wang, Wei Wang, Xing Xu, Wu-Zhou Huang, Jin-Peng Zhang, Yong-Wei Liu, Xiao-Fei Ma, Jing-Na Ru, Yun-Feng Jiang, Jun Chen, Xiu-Liang Zhu, Yong-Bin Zhou, Ming Chen, Xin-You Cao, Shuang-Xi Zhang, Guo-Yue Chen, Li-Hui Li, You-Zhi Ma & Zhao-Shi Xu

TaMPK3 Mediates Synergistic Damage from *Fusarium* Crown Rot and Drought in Wheat

Lei Zheng[1,†], Tai-Fei Yu[1,†], Ying Liu[1,†], Ze-Hao Hou[1,†], Ji-Tong Wei[1], Jia-Min Hao[1], Xing-Yu Liu[1], Xin-Rui Wang[1], Wei Wang[1], Xing Xu[1], Wu-Zhou Huang[1], Jin-Peng Zhang[1], Yong-Wei Liu[2], Xiao-Fei Ma[3], Jing-Na Ru[3], Yun-Feng Jiang[4], Jun Chen[1], Xiu-Liang Zhu[1], Yong-Bin Zhou[1], Ming Chen[1], Xin-You Cao[5], Shuang-Xi Zhang[6], Guo-Yue Chen[4], Li-Hui Li[1,7], You-Zhi Ma[1,7], and Zhao-Shi Xu[1,7*]

[1] State Key Laboratory of Crop Gene Resources and Breeding, Institute of Crop Sciences, Chinese Academy of Agricultural Sciences (CAAS), Beijing 100081, China

[2] Institute of Biotechnology and Food Science, Hebei Academy of Agriculture and Forestry Sciences/Hebei Key Laboratory of Drought-Alkali Tolerance in Wheat, Shijiazhuang 050051, China

[3] Institute of Wheat Research/The Industrial Crop Institute, Shanxi Agricultural University, Taiyuan 030000, China

[4] Triticeae Research Institute, Sichuan Agricultural University, Chengdu 611130, China

[5] National Engineering Laboratory for Wheat and Maize/Key Laboratory of Wheat Biology and Genetic Improvement, Crop Research Institute, Shandong Academy of Agricultural Sciences, Jinan 250100, China

[6] Institute of Crop Science, Ningxia Academy of Agriculture and Forestry Sciences, Yongning 750105, China

[7] National Nanfan Research Institute (Sanya), Chinese Academy of Agricultural Sciences/Seed Industry Laboratory, Sanya 572024, China

[†] These authors contributed equally to this work.

[*] Correspondence: Zhao-Shi Xu (xuzhaoshi@caas.cn)

Abstract

Fusarium crown rot (FCR) is a hard-to-control wheat disease prevalent in arid and semi-arid regions. However, the relationship between arid conditions and FCR disease remains unclear. Here, we confirm that drought stress exacerbates the severity of FCR, and that FCR intensifies drought-induced damage. Integrated transcriptome analysis indicates that *TaMPK3* gene exhibits distinctly opposite expression patterns under these two stress conditions. Functional identification verifies that *TaMPK3* positively regulate FCR resistance while negatively influencing drought tolerance. Upon *TaMPK3* gene knockout, the mutually reinforcing effect between drought and FCR is eliminated. TaMPK3 is found to modulate TaWRKY26 activity to regulate the expression of sterol synthesis gene clusters, thereby influencing FCR resistance. Within this cluster, the key gene *TaCYP51H37* significantly enhances FCR resistance. Combined with our findings that TaMPK3 decreases drought tolerance through ABA signaling pathway, this study proposes a molecular model in which TaMPK3 mediates the synergistic damage caused by drought and FCR.

Introduction

Fusarium crown rot (FCR), a soil-borne disease, inflicts significant damage on wheat and barley. This disease is highly prevalent in arid and semi-arid regions, resulting in substantial plant lodging, mortality, and yield reduction. Furthermore, contamination of grain with deoxynivalenol (DON), nivalenol (NIV), and other mycotoxins produced by the FCR pathogen substantially increases the health risks associated with wheat consumption[1]. FCR was first documented in Australia in 1951[2] and was subsequently identified in major wheat-producing regions across Asia, Africa, the Americas, and the Middle East[3,4,5]. The recent expansion of FCR-affected areas has rendered the management and control of this disease an urgent challenge in wheat production. An effective strategy for controlling FCR was identified as one of the top ten industrial issues raised at the 24th Annual Meeting of the China Association for Science and Technology in 2022.

The primary pathogen responsible for FCR is *Fusarium pseudograminearum* (*Fpg*). Additional *Fusarium* species, such as *F. graminearum* (*Fg*), *F. culmorum* (*Fc*), and *F. proliferatum*

(*Fpr*), are also commonly found[6,7]. *Fusarium* spp. are capable of persisting in soil for extended periods. Research has demonstrated that *Fpg* remains viable in crop residues for up to three years[8,9,10]. The symptoms of FCR are difficult to detect during the early stages of infection. However, once the infection is established, the growth of *Fpg* can proceed extremely rapid[11,12,13]. Furthermore, the duration of the damage caused by FCR is prolonged, as it can affect plants from the seedling stage through to adult stage[14,15,16]. Consequently, FCR poses substantial challenges for the management of wheat fields. Breeding resistant varieties is potentially the most economical and effective strategy for controlling FCR. It is crucial to focus research on the discovery and development of resistant germplasm, as well as on gaining a comprehensive understanding of the genes involved and the underlying mechanisms.

Extensive screening has been conducted to identify wheat germplasm that harbors resistance to FCR. However, only a limited number of moderately resistant cultivars have been identified, and no cultivar exhibiting high resistance or immunity to FCR has been reported. These findings indicate that the majority of widely cultivated modern cultivars exhibit either susceptible or highly susceptible to FCR[17,18,19,20]. By leveraging high-throughput sequencing technology, several quantitative trait loci (QTL) associated with FCR resistance have been identified on chromosomes 1B, 2A, 3D, 5D, and 6A[21,22,23,24,25]. However, a comprehensive understanding of the genes involved in regulating FCR resistance and their regulatory mechanisms remains limited. A genome-wide association study (GWAS) conducted by Yang et al. identified *TaDIR-B1* as the gene associated with FCR resistance[26]. The *TaCWI-B1* gene was identified in 2023 using BSR-seq (Barcode splitting reads sequencing) analysis. This gene influenced FCR resistance by modulating thickness and composition of the cell wall[27]. A transcriptomic sequencing study pinpointed the *TaRLK-6A* gene differentially expressed in both resistant varieties and sensitive varieties[28]. An integrative analysis of transcriptomics and metabolomics has pinpointed a tryptophan metabolic pathway that contributed to FCR resistance. Key synthesis-regulated genes *TaALDHase*, *TaWRKY24*, and *TaMTase* involved in the tryptophan metabolic pathway were identified to play significant roles in influencing FCR response[29]. A GWAS and whole-exome sequencing (WES)

identified a catalase antioxidant enzyme gene, *TaCAT2*, which is associated with FCR resistance. Further investigations revealed that TaSnRK1α phosphorylates TaCAT2 and mediates resistance to FCR[30]. The *TaHSP18.6* gene was identified through the integration of transcriptome analysis and GWAS. The TaHSP18.6 proteins was verified to interact with TaSRT1 and to regulate FCR resistance by mediating the *TaIAA1* gene to modulate the endogenous auxin content in wheat[31].

During the field management process, it was discovered that drought could exacerbate the severity of FCR. Nevertheless, research dedicated to exploring the relationship between drought and FCR remains scarce. In 2016, it was confirmed that drought prolongs the initial infection phase but enhances the proliferation and spread of *Fusarium* pathogens after the initial infection phase in barley[32]. Su et al. identified a significant overlap between the DEGs induced by FCR and those triggered by drought stress[33]. In 2022, research confirmed that yield losses caused by FCR were strongly correlated with water conditions during the flowering and grain-filling stages. FCR could decrease water use efficiency in wheat and lead to greater yield reductions[34]. Su et al. generated a pair of near isogenic lines (NILs) that exhibited significant differences between the two lines in both FCR resistance and drought tolerance. Transcriptomic analysis of these two lines demonstrated that similar regulatory frameworks were activated in coping with FCR and drought stresses[35].

A comprehensive comprehension of the mechanisms underlying the interaction between drought stress and FCR symptoms is crucial for the effective prevention and management of FCR. In this study, the severity of FCR was examined through stem surface inoculation and stem internal injection under both drought and normal conditions. Regardless of the inoculation method employed, the severity of FCR under drought conditions was significantly higher than that under normal conditions. This finding verified that, compared with the impact of the soil environment on *Fpg*, the alterations in the physiological state of wheat under drought stress were the critical factor leading to the exacerbation of FCR. Combined transcriptome analysis of wheat under drought treatment and *Fpg* infection revealed that the DEGs were significantly enriched in the mitogen-activated protein kinase (MAPK) signaling pathway. Within this pathway, the key gene

TaMPK3 showed the most pronounced expression differences under drought conditions and *Fpg* infection. Based on the *TaMPK3* gene, we investigated the molecular mechanism underlying the synergistic damage inflicted by drought and FCR in wheat. This research elucidates the significant influence of drought on the severity of FCR and the associated molecular mechanisms. Consequently, it provides a crucial molecular foundation for the molecular design breeding of FCR-resistant varieties.

Results

Drought inhibits the expression of genes in the MAPK signaling pathway that responds to FCR infection

To identify the cause of the high incidence of FCR in wheat under drought conditions, we evaluated FCR disease indices by conducting stem surface inoculation with diseased wheat kernels and stem internal infection by injecting spore suspensions in both drought and normal growth environments (Figure 1 a and d). After both types of infection, disease indices under drought conditions were all significantly higher than those in normal environments. Moreover, the effect of drought on disease indices was similar between the two inoculation methods (Figure 1 b-c and e-f). This finding indicated that alterations in the physiological state of wheat critically contribute to the exacerbation of FCR under drought conditions.

The transcriptomes analyzed at 0, 2, and 4 days post *Fpg* infection revealed 5,875 common differentially expressed genes (DEGs) that were up-regulated at both 2 and 4 days after *Fpg* infection. Among them, 762 DEGs overlapped with the DEGs that were down-regulated under drought treatment. In contrast, only 26 common DEGs were down-regulated upon *Fpg* infection and up-regulated under drought conditions (Figure 1 g). Under drought stress and *Fpg* infection, there were 189 common up-regulated DEGs and 149 common down-regulated DEGs (Supplemental Fig.1 a-c). These findings suggested that drought suppressed the expression of certain genes associated with FCR response. Gene Ontology (GO) and Kyoto Encyclopedia of Genes and Genomes (KEGG) enrichment analysis were conducted on 762 DEGs that were up-

regulated during *Fpg* infection and down-regulated under drought conditions. The result demonstrated that these genes were significantly enriched in multiple metabolic and biosynthetic pathways, with the MAPK signaling pathway exhibiting a particularly high level of enrichment (Figure 1 h and Supplemental Fig.2). The components of the MAPK signaling pathway that respond to pathogen infection, including the receptor protein FLS2, members of the MAPK cascade (MEKK, MKK, and MPK), and the WRKY transcription factor, were all up-regulated in response to FCR and down-regulated under drought stress. Notably, the *Mitogen-activated protein kinase 3* (*MPK3*) and *TaWRKY26* genes exhibited the most pronounced up-regulation in response to FCR (Figure 1 i and j). Quantitative analysis of the stem base revealed that *Fpg* infection led to up-regulation of *TaMPK3* genes expression, whereas drought significantly suppressed their up-regulation expression (Figure 1 k-m). We assessed *TaMPK3* gene expression levels under drought stress and FCR infection in key cultivated varieties, revealing that differential expression of *TaMPK3* under these two stress conditions is a widespread occurrence (Supplemental Fig.3 a-b). Moreover, TaMPK3 protein abundance was markedly elevated under FCR infection (Supplemental Fig.3 c).

TaMPK3 positively regulated FCR resistance but negatively affected drought tolerance in wheat

Tissue expression pattern analysis revealed that *TaMPK3* genes were mainly expressed in the roots, stems, and leaves at both the seedling and adult stages. The highest expression level was detected in the leaves and leaf sheaths (Supplemental Fig.4 a). Both overexpression and gene-edited lines of *TaMPK3* gene were generated in the cultivar Fielder for functional analysis. Three gene-edited lines were identified as triple mutants, each harboring single-base insertions or deletions in the coding sequence of the Pkinase domain (Figure 2 a and Supplemental Fig.4 b). These single-base alterations led to frameshifts and premature termination codons (Supplemental Fig.5). Quantitative analysis demonstrated a significant increase in *TaMPK3* expression in overexpression lines (*TaMPK3*-OE), whereas the mRNA of *TaMPK3* genes were substantially reduced in gene-edited lines (*TaMPK3*-KO) (Figure 2 d). The observed abundance of the TaMPK3

protein corresponds to the quantified expression level of the *TaMPK3* gene (Supplemental Fig.6). *TaMPK3*-OE, *TaMPK3*-KO, and wild-type (WT) lines were planted for ten days and then inoculated with *Fpg*. Thirty days post-inoculation, the *TaMPK3*-OE lines exhibited significantly enhanced resistance to FCR, with a decrease in disease indices. In contrast, the *TaMPK3*-KO lines displayed more severe disease symptoms compared to the WT (Figure 2 b-c and e). Shoot length statistics for plants grown under normal conditions indicated that *TaMPK3*-OE lines had significantly shorter shoots compared to the WT, while the *TaMPK3*-KO lines showed an increasing trend. Under *Fpg* infection, the shoot length of *TaMPK3*-OE lines decreased slightly but remained significantly higher than that of the WT, whereas the *TaMPK3*-KO lines displayed a substantial reduction (Figure 2 f). Under normal conditions, the fresh weight and dry weight of shoots in *TaMPK3*-OE lines were significantly lower than those of the WT, whereas no significant difference was observed between *TaMPK3*-KO lines and WT plants. Following *Fpg* infection, the fresh weight and dry weight of *TaMPK3*-OE lines were significantly higher than those of WT plants. Conversely, the fresh weight and dry weight of the *TaMPK3*-KO lines were significantly lower (Figure 2 g-h).

The growth status of *TaMPK3*-OE, *TaMPK3*-KO, and WT seedlings were evaluated under drought conditions. After 20 days of water-deficit treatment, the *TaMPK3*-OE lines displayed pronounced wilting, whereas the *TaMPK3*-KO lines maintained a healthier growth status compared to the WT. Following 5 days of rehydration, the *TaMPK3*-KO lines recovered to near-normal growth, whereas the *TaMPK3*-OE lines showed a markedly higher mortality rates relative to the WT (Figure 3 a). Dry weight, catalase (CAT) activity, malondialdehyde (MDA) content, and proline (PRO) content were measured. The results indicated that the *TaMPK3*-OE lines significantly suppressed plant growth under drought stress, with a reduced shoot dry weight; exacerbated cellular damage, markedly increased MDA levels; significantly decreased CAT activity, diminished cellular antioxidant capacity; and significantly reduced PRO content, weakening osmotic regulation ability. In contrast, the *TaMPK3*-KO lines exhibited enhanced drought tolerance compared to the WT plants. The *TaMPK3*-KO lines showed increased shoot dry

weight, significantly reduced MDA level, markedly elevated CAT activity, and higher PRO content (Figure 3 b-e). Under normal field conditions, the growth status and yield of transgenic lines and WT plants were evaluated. With the exception of a decrease in plant height in the *TaMPK3*-OE lines, no differences were observed in yield traits between the transgenic lines and the WT, including panicle length, spike number, thousand grain weight, grain weight per plant, grain length, and grain width. Under drought stress conditions, grain width, thousand grain weight, and grain weight per plant were significantly reduced in the *TaMPK3*-OE lines. In contrast, the *TaMPK3*-KO lines exhibited increased grain width and grain weight per plant; however, these increases were not statistically significant (Figure 3 f-k and Supplemental Fig.7 a-d).

The *TaMPK3* gene modulates the inhibitory effect on *Fpg* growth in wheat

Infection of the stem base wounds of the *TaMPK3*-OE, *TaMPK3*-KO, and WT lines with *Fpg* spore suspensions resulted in browning of the surrounding tissues. The browning degree in the *TaMPK3*-OE lines was significantly lower than that of WT. Conversely, the *TaMPK3*-KO lines exhibited pronounced browning (Figure 4 a). Staining with Trypan Blue solution revealed profuse mycelia growth at the wounds of *TaMPK3*-KO plants compared to the WT, whereas less mycelia development was observed on *TaMPK3*-OE plants (Figure 4 b). The wheat germ agglutinin (WGA) fluorescence staining results indicated that the stem bases of *TaMPK3*-KO plants exhibited significantly higher levels of mycelia fluorescence compared to those of the WT and *TaMPK3*-OE lines (Figure 4 c). The extracts from the stem base of the *TaMPK3*-OE, *TaMPK3*-KO, and WT lines were prepared and added to the culture medium to assess their effects on the growth of *Fpg*. On the potato dextrose agar (PDA) medium, at concentrations of 0.8 mg/mL and 1.6 mg/mL, the extracts significantly inhibited mycelial growth (Supplemental Fig.8 a-b). The extracts from the stem base of the *TaMPK3*-OE lines had greater inhibitory effects on *Fpg* mycelia growth than those from the WT, while the inhibitory effects of the extracts from the *TaMPK3*-KO lines was significantly decreased (Figure 4 d-e). The inhibitory effects of extracts from *TaMPK3*-OE, *TaMPK3*-KO and WT lines, when added to the sodium carboxymethylcellulose (CMC) medium, were consistent with those observed on PDA medium (Figure 4 f-g). These results demonstrated

that the *TaMPK3* gene may have an effect on *Fpg* growth suppression by modulating specific metabolites in planta.

The expression of the sterol synthesis gene clusters was regulated by TaMPK3

Analysis of transcriptome data from *TaMPK3*-OE and *TaMPK3*-KO lines revealed that 849 genes had significantly increased expression in the *TaMPK3*-OE lines compared to the *TaMPK3*-KO lines. Among them, 366 genes overlapped with the genes that were up-regulated in response to *Fpg* infection (Figure 5 a). The GO and KEGG enrichment analyses of these DEGs indicated that the FCR-related genes regulated by *TaMPK3* were primarily enriched in secondary metabolite biosynthesis pathways. The sterol synthesis pathway exhibited the highest enrichment factor values (Figure 5 b-d). Intriguingly, the genes encoding the sterol biosynthesis pathway were identified to be localized in adjacent regions on chromosomes 5A and 5D, forming distinct gene clusters (Figure 5 e). In 2022, Polturak et al. identified that this sterol synthesis gene cluster catalyzes the production of a novel terpenoid compound, ellarinacin, which responds to pathogen-induced stress[36] (Figure 5 f). Quantitative analysis of stem base tissues showed that the expression of sterol synthesis genes were significantly up-regulated in *TaMPK3*-OE lines and down-regulated in *TaMPK3*-KO lines (Figure 5 g-q). Under normal conditions, the expression levels of sterol synthesis genes were extremely low in wheat. However, they were significantly up-regulated following infection by *Fpg* (Supplemental Fig.9).

The *TaCYP51H37* gene improves FCR resistance and drought tolerance in wheat

The TaCYP51H37 protein catalyzes the final step of ellarinacin synthesis, and its expression showed the most significant response to FCR and TaMPK3 regulation (Figure 5 d, f, i and o). We generated overexpression lines of the *TaCYP51H37* gene and selected three lines for gene function analysis (Figure 6 a-b and Supplemental Fig.10). The *TaCYP51H37*-OE lines exhibited a significantly enhanced resistance to FCR (Figure 6 a and c-d). Under normal growth conditions, there were no significant differences in shoot length, fresh weight, and dry weight between the *TaCYP51H37*-OE lines and the WT plant; upon *Fpg* infection, the shoot length, fresh weight, and dry weight of the *TaCYP51H37*-OE lines were significantly higher than those of the WT (Figure

6 e-g). Silencing of *TaCYP51H37* gene resulted in significantly reduced FCR resistance (Supplemental Fig.11 a-e). The plant height, dry weight, and fresh weight were decreased compared to those of the control BSMV: γ lines (Supplemental Fig.11 f-h). The browning degree of wound sites on the stem base of *TaCYP51H37*-OE lines was significantly reduced compared with that of the WT lines (Figure 6 h). The *Fpg* mycelia in the stem base of *TaCYP51H37*-OE lines were significantly decreased compared with those in the WT lines (Figure 6 i and Supplemental Fig.12). The growth rate of *Fpg* on the PDA medium (Figure 6 j-k) and in the CMC medium (Figure 6 l-m) containing extracts from *TaCYP51H37*-OE lines was significantly lower than that on the medium containing extracts from WT plants.

The *TaCYP51H37*-OE lines exhibited enhanced drought tolerance in seedling stage tests (Supplemental Fig.13 a). Under drought conditions, the shoot weight of *TaCYP51H37*-OE plants was significantly higher than that of WT plants. The contents of CAT and PRO were markedly increased, and the content of MDA was significantly reduced in *TaCYP51H37*-OE plants compared to WT plants (Supplemental Fig.13 b-e). Under both normal and drought conditions in the field, no significant differences were observed in plant height, grain length, grain width, or grain weight between *TaCYP51H37*-OE plants and WT plants, except that an increase in the spike number and grain weight per plant was noted in the *TaCYP51H37*-OE plants grown under drought conditions (Supplemental Fig.13 f-m). However, VIGS-mediated silencing of *TaCYP51H37* did not significantly alter drought tolerance in wheat (Supplemental Fig.11 i-m).

TaMPK3 regulates the expression of sterol synthesis gene clusters by phosphorylating TaWRKY26 transcription factors

Through co-expression network analysis, transcription factors associated with the expression of sterol synthesis gene clusters were screened (Supplemental Fig.14 a-b). The result indicated that the transcription factors co-expressed with the sterol synthesis genes included WRKY, bHLH, HsfA, NAC, and CHR (Figure 7 a). Using yeast two-hybrid assays to detect the interaction between these transcription factors and TaMPK3 protein, TaWRKY26, TaWRKY50, TaWRKY51, and TaWRKY72 transcription factors were verified to interact with TaMPK3 protein (Figure 7 b).

Bimolecular fluorescence complementation (BIFC) and luciferase complementation imaging (LCI) assays were conducted to confirm these interactions in tobacco (Figure 7 c-d and Supplemental Fig.15). Additionally, the interaction between the TaMPK3 and these TaWRKY transcription factors was verified through pull-down assay *in vitro* (Figure 7 e).

The autophosphorylation activity of the TaMPK3 protein was detected via the Phos-tag method (Supplemental Fig.16). The TaWRKY26 transcription factor was verified to be phosphorylated by TaMPK3 (Figure 8 a), and its expression was significantly induced by *Fpg* infection in the stem base of wheat (Figure 1 j and Supplemental Fig.17). Transcription factor binding site analysis revealed a substantial number of WRKY binding sites within the 2000 bp promoter regions of sterol synthesis genes (Supplemental Fig.18). The bindings of the TaWRKY26 protein to the promoter regions of the sterol synthesis genes were confirmed through yeast one-hybrid assays (Figure 8 b). Electrophoretic mobility shift assays (EMSA) confirmed that TaWRKY26 binds to WRKY binding site segments within the promoters of these sterol synthesis genes (Figure 8 c). The promoter regions of the sterol synthesis genes were inserted upstream of the vector containing luciferase (LUC) reporter gene (Figure 8 d). Dual-LUC reporter assays were employed to identify the activation of the promoters of the sterol synthesis genes by TaWRKY26 transcription factors. Furthermore, the TaMPK3 protein was verified to significantly enhance the transcriptional regulatory effect of TaWRKY26 on the sterol synthesis genes in wheat protoplasts and tobacco (Figure 8 e-f). In the absence of TaWRKY26, the TaMPK3 protein failed to activate the promoter region of sterol synthesis genes (Supplemental Fig.19). VIGS-mediated silencing of *TaWRKY26* genes led to an increase in FCR symptoms (Supplemental Fig.20 a-e). Plant height, dry weight, and fresh weight were all markedly decreased compared to those of the control lines (Supplemental Fig.20 f-h). In contrast, silencing the *TaWRKY26* gene did not significantly alter the drought tolerance of wheat (Supplemental Fig.20 i-m).

TaMPK3 mediated the reduced drought tolerance caused by *Fpg* and the decreased FCR resistance under drought conditions

The expression of *TaMPK3* was significantly up-regulated following *Fpg* infection. Moreover,

overexpression of *TaMPK3* led to a reduction in drought tolerance. To verify whether *Fpg* infection impacts the drought tolerance of wheat, *Fpg* spore suspensions were injected into wheat stem base when the plants started to exhibit drought symptoms under water-controlled conditions. Five days post-injection, it was observed that the drought sensitivity of the injected WT plants increased significantly (Figure 9 a). The shoots exhibited substantial wilting, and the fresh weight of shoots decreased significantly. Additionally, there were remarkable increases in MDA content, CAT activity, and Pro content (Figure 9 b). The *TaMPK3*-OE lines exhibited a phenotype similar to that of WT plants (Figure 9 c-d). Interestingly, in *TaMPK3*-KO lines, the enhancement effect of *Fpg* infection on drought damage was abolished. No significant differences were observed between the *Fpg*-injected groups and the non-injected groups (Figure 9 e-f). The *TaCYP51H37*-OE lines exhibited increased drought sensitivity under *Fpg* treatment. However, the difference between *Fpg*-treated groups and control groups was less pronounced than that observed in the WT and *TaMPK3*-OE lines. This may be attributed to the *TaCYP51H37* gene conferring resistance to FCR and drought (Figure 9 g-h).

The enhancement effect of *Fpg* infection on drought damage was eliminated when the *TaMPK3* genes were knockout in wheat. To investigate whether the *TaMPK3* gene also influences the drought effect on FCR resistance, *TaMPK3*-OE, *TaMPK3*-KO, and *TaCYP51H37*-OE lines were inoculated with *Fpg* under both drought and normal growth conditions (Figure 9 i, k and m). The FCR disease indices of *TaMPK3*-OE lines under drought conditions were significantly higher than those under normal conditions (Figure 9 j), showing a trend similar to that observed in the WT plants (Figure 1 c and f). Notable, in *TaMPK3*-KO lines, the negative impact of drought on FCR resistance was also mitigated (Figure 9 k-l). In *TaCYP51H37*-OE lines, the FCR disease indices were higher under drought conditions compared to normal conditions, but the difference was less pronounced than that observed in WT and *TaMPK3*-OE lines (Figure 9 m-n). These results demonstrated a synergistic interaction between drought and FCR stress in wheat, in which the *TaMPK3* genes play a pivotal role.

In our previous findings, TaMPK3 decreased drought tolerance through interacting with the

ABA signaling receptor TaPYL4 and promoting its degradation[37]. We investigated the influence of the *TaMPK3* gene on the expression of reported downstream effector genes of PYL in wheat, and found that their expression was substantially up-regulated in *TaMPK3*-KO lines (Supplemental Fig.21 a). Subsequently, we examined whether the reported downstream effector genes of TaPYL were affected by FCR. The results showed that the expression levels of *TaPYL1-1B*, *TaSLAC1*, and *TaCAT1* genes were significantly downregulated under *Fpg* infection, while the expression of the *TaASR2L* gene was markedly up-regulated (Supplemental Fig.21 c). In contrast, the expression levels of these genes exhibited minimal difference in TaWRKY26-silenced lines and TaCYP51H37-OE lines (Supplemental Fig.21 e and g). These findings indicate that FCR modulates drought tolerance through the interaction between TaMPK3 and TaPYL, independently of the TaWRKY26 and TaCYP51H37 mediated regulatory pathways involved in FCR resistance. The upregulation of the *TaASR2L* gene may respond to *Fpg* infection via other pathways. The molecular model was established to explain the synergistic damage caused by drought and FCR, which is mediated by TaMPK3 protein (Figure 10).

Discussion

Over the past years, FCR has exhibited a rapidly increasing trend in the primary wheat-producing regions of the Huanghuai area in China, particularly in the arid and semi-arid regions, posing a significant threat to both wheat yield and quality[30,35]. However, the scarcity of wheat resources with high resistance to FCR has impeded the identification of resistance genes and the development of FCR-resistant wheat varieties[21,22]. Although functional genes regulating wheat resistance to FCR, such as *TaCWI*[27], *TaRLK-6A*[28], and *TaCAT2*[30], have been identified, the genetic improvement of FCR-resistant wheat varieties still faces significant challenges due to the limited availability of known functional genes and molecular mechanisms. Notably, research has shown that drought stress exacerbates FCR infection in wheat[32,33,34,35]. Indeed, our findings demonstrate that drought and FCR act synergistically, leading to compounded damage. FCR substantially compromises wheat's drought tolerance, increasing its susceptibility to stress (Figure 9 a-b), while

drought impairs wheat's resistance to FCR, thereby markedly exacerbating disease severity (Figure 1 a-f). These findings further clarify the underlying reasons for the prevalence of FCR in arid and semi-arid regions. Therefore, analyzing the molecular crosstalk between these stress responses and disrupting their shared regulatory pathways may provide novel strategies for enhancing wheat resistance to FCR.

Interestingly, transcriptome analysis revealed that the *TaMPK3* gene exhibits contrasting expression patterns under drought stress and FCR infection conditions (Figure 1 j-m). It functions as a positive regulator of FCR resistance in wheat, while acting as a negative regulator of drought tolerance (Figure 2 and Figure 3). Importantly, the synergistic interaction between drought stress and FCR response was abolished following *TaMPK3* gene knockout (Figure 9 e-f and k-i). This result suggests that TaMPK3 functions as a key node in the regulatory network connecting drought and FCR responses. MPKs are critical components of the MAPK cascade and play pivotal roles in regulating diverse biological processes, particularly plant immunity[41]. In wheat, TaMPK4 has been demonstrated to positively regulate the plant's response to abiotic stresses, including phosphorus and nitrogen deficiency as well as high salinity[42]. TaMPK6 participates in the regulation of immunity by modulating the activation of the immune component TaSGT1[43]. Our findings reveal that TaMPK3 promotes the FCR response by enhancing the transcriptional activity of TaWRKY26 (Figure 8 and Figure 10). Moreover, previous studies have shown that the MPK3 is involved simultaneously in both biotic and abiotic stress response pathways. In Arabidopsis, MPK3 contributes to the robustness of effector-triggered immunity (ETI) by promoting reactive oxygen species (ROS) accumulation and hypersensitive response (HR)-associated cell death[44]; it also suppresses lateral root development in response to drought through phosphorylation-mediated degradation of the IAA15 protein[45]. In our study, TaMPK3 was identified not only as a regulator of FCR resistance but also as a negative regulator of drought tolerance, acting through destabilization of TaPYL4 and consequent impairment of ABA signaling[37]. Collectively, these results indicate that MPK3 plays a dual regulatory role in drought tolerance and disease resistance, representing a key signaling node where the two stress response pathways intersect, and further

identify a TaMPK3–TaWRKY26 molecular module involved in regulating FCR resistance in wheat. Notably, we discovered that, unlike *TaMPK3*, silencing of *TaWRKY26* gene did not to affect the downstream effector genes of the ABA signal transduction pathway (Supplemental Fig.21 e and f). This finding suggests that TaMPK3 regulates drought tolerance and FCR resistance in wheat through two distinct and independent signaling pathways.

Additionally, a recent study has demonstrated that the expression of sterol biosynthesis gene clusters is associated with wheat disease resistance and that these genes are involved in catalyzing the synthesis of a novel sterol compound, ellarinacin[36]. Our result revealed that these sterol biosynthesis gene clusters were downstream of the TaMPK3-TaWRKY26 module (Figure 8 and Figure 10). Overexpression the ellarinacin biosynthesis enzyme *TaCYP51H37* enhances wheat resistance to FCR, and plant extracts from *TaCYP51H37*-OE lines suppress *Fpg* growth within plants. (Figure 6). Furthermore, silencing *TaCYP51H37* (Supplemental Fig.11 a-h) and other genes (*TaOSC*, *TaCYP51H35*, and *TaHSD*) in sterol biosynthesis-related gene cluster resulted in a significant reduction in FCR resistance in wheat (Supplemental Fig.22-24). Our results revealed that sterol compounds are involved in the FCR response in wheat. Notably, in soybean, enhancing sterol biosynthesis or the exogenous application of these compounds can improve crop tolerance to drought stress through their antioxidant effects[46]. The accumulation of cholesterol, a homologue of ellarinacin, leads to dwarfism and improved drought tolerance in herbaceous plants[47]. Similarly, we also discovered that overexpression of *TaCYP51H37* conferred drought tolerance to wheat (Supplemental Fig.13). These results reveal that these sterol compounds are also involved in plant responses to abiotic stress. Interestingly, overexpression of *TaMPK3* in wheat leads to elevated expression of *TaCYP51H37.* However, high expression of *TaCYP51H37* does not confer strong drought tolerance on *TaMPK3*-overexpressing plants. Further analysis indicated that, unlike that of *TaMPK3*, the overexpression of *TaCYP51H37* does not influence the ABA signal pathway (Supplemental Fig.21 e). Moreover, silencing of sterol biosynthesis genes did not affect wheat's tolerance to drought stress (Supplemental Figure 11 i-m and Supplemental Figure 22–24). Silencing *TaCYP51H37* in *TaMPK3*-overexpressing plants did not significantly alter plant

tolerance to drought stress (Supplemental Figure 25 a–g), whereas silencing *TaMPK3* in *TaCYP51H37*-overexpressing plants significantly enhanced tolerance to drought stress (Supplemental Figure 25 h–n). These results further confirm that the TaMPK3-mediated sterol biosynthesis pathway is independent of its negative regulation of wheat drought stress tolerance.

Since the initial identification of FCR in China in 2011, no cultivars exhibiting high levels of resistance have been reported[21,22]. *TaCAT2*, which was identified through an analysis of natural variation among 243 Chinese wheat accessions, has the potential to enhance wheat resistance to FCR[30]. We observed that the expression of *TaCAT2* was markedly up-regulated in *TaMPK3*-OE lines and upon FCR infection (Supplemental Fig.21 b and d), further underscoring the importance of *TaMPK3* in mediating wheat resistance to FCR. However, analysis of natural variation in *TaMPK3* reveals a severe limitation in genetic diversity within its coding and promoter regions (Supplemental Fig.26), thereby resulting in the absence of natural germplasms that can eliminate the synergistic damage induced by drought and FCR. This may be a key factor contributing to the difficulty in identifying highly resistant germplasm resources for FCR. The *TaWRKY26* gene on chromosomes 1B and 1D also exhibited limited natural variation, while the *TaWRKY26-1A* allele harbors a significantly higher level of genetic variation in wheat (Supplemental Fig.27), suggesting its potential as a candidate gene for conferring wheat resistance to FCR. Furthermore, collinear analysis revealed that multiple copies of the sterol synthesis gene cluster are present on the wheat chromosome (Supplemental Fig.28 a); however, these copies were not expressed under either normal or *Fpg* infection (Supplemental Fig.28 d). Structural characteristic analysis suggests that although the promoter regions of these homologous genes contain WRKY binding sites, large fragment insertions in their 5′UTR regions may account for their extremely low expression levels (Supplementary Figure 28 b–c). Interestingly, natural variation within sterol synthesis gene clusters on wheat chromosomes is constrained (Supplementary Figure 29-30), while their homologous copies exhibit relatively higher genetic diversity (Supplementary Figure 31-33). Consequently, the identification and exploitation of superior allelic variants from these homologous genes may advance the development of FCR-resistant genes and wheat varieties.

In conclusion, we have elucidated the molecular mechanism underlying the damage caused by the synergistic effects of FCR and drought stress in wheat, and have identified TaMPK3 as a critical nexus integrating the signaling pathways of these two stresses. In addition, our findings reveal that the TaMPK3–TaWRKY26 module plays a critical role in regulating wheat resistance to FCR by promoting the sterol biosynthesis pathway. Notably, we found that knockout of TaMPK3 disrupts the mutual enhancement between drought and FCR, and significantly enhances drought tolerance in wheat without compromising yield-related traits. Therefore, we propose a valuable breeding strategy that specifically inhibits TaMPK3 to disrupt the drought–FCR interaction while simultaneously upregulating downstream effector genes (*TaWRKY26*, *TaCAT2*, and sterol gene cluster), potentially enabling the rapid improvement of wheat varieties with enhanced resistance to FCR.

Methods

Plant materials and growing conditions

The wheat plants were grown in a culture room at 50% relative humidity, with a photoperiod of 16 h of light at 25 ℃ and 8 h of darkness at 18 ℃. The mid-resistant wheat variety PuBingZi300 (PBZ300) was used for transcriptome sequencing analysis under FCR stress. The wheat variety Fielder (wild-type, WT) was utilized for transcriptome sequencing analysis under drought conditions, generating of transgenic wheat lines, gene cloning, and assessing FCR resistance under both normal and drought conditions. *Nicotiana benthamiana* was used for BIFC, LCI and dual-LUC reporter assays. Stress-tolerant wheat varieties (including Pinyu 8012, Zhengmai 1860, Jimai 60, Jinhe 991 and Ningmai 58) were selected for gene cloning to identify sequence variations and quantify gene expression.

Generation of transgenic wheat

Full-length coding DNA sequences (CDS) of the *TaMPK3* (TraesCS4D02G198600) and *TaCYP51H37* (TraesCS5A02G004700) genes were cloned into the plant transformation vector *pWMB110* containing the maize ubiquitin promoter. The Pkinese domain sequence in *TaMPK3*

was analyzed using CRISPR-P 2.0 web tools to design an sgRNA (single guide RNA) sequence, which was cloned into the pBUE411 vector CRISPR (Clustered Regularly Interspaced Short Palindromic Repeats) system for generating gene-edited wheat. The recombinant vectors were introduced into the host plants via *Agrobacterium*-mediated transformation. DNA was extracted from putative transformed lines to confirm positive transgenic lines, and RNA was extracted to quantify gene expression level. Third-generation transgenic wheat lines were used for phenotypic analysis. All primers are listed in Supplementary Data 1.

Propagation and inoculation of *Fpg*, and disease grades for assessing FCR damage

Mycelial cultures of *Fpg* were grown on potato dextrose agar (PDA) solid medium, and spores were produced in carboxymethylcellulose (CMC) liquid medium. To produce diseased wheat kernels, *Fpg* was cultured on PDA medium at 25°C for 5 days and then mixed with steamed wheat kernels and incubated at 25°C for 10 days. To prepare spores for inoculation, *Fpg* was transferred from PDA medium to CMC medium and shaken at 28°C and 180 r/min for 5-7 days. The spores were collected by filtration, and the concentration was adjusted to 1×10^6 spores/mL for inoculation of wheat plants.

The severity of FCR damage was assessed using a 0-6 scale, which incorporated a new grade inserted between grades 3 and 4 of the previous 0-5 scale system[48]. This additional grade specifically corresponds to the occurrence of lesion spots on the third leaf sheath and severe necrotic lesions on the second leaf sheath. A disease index (DI) was calculated according to the formula: $(\Sigma nX / 6N) \times 100$, where X represents the disease severity score, n denotes the number of plants assigned to a given score, and N is the total number of plants evaluated.

Drought treatments

For drought treatment at the seedling stage, pots were filled with 245g of uniformly moist soil. Six germinated wheat grains were planted and covered with additional moist soil (25g). The seedlings were placed in an incubator, and no additional water was supplied during the experiment. On the 20th day of drought treatment, the plants were rewatered. Five days after rewatering, growth status and physiological parameters were assessed. Each drought treatment experiment consisted

of three replicates, and the physiological indicators of each genotype were measured in triplicate.

Wheat lines were grown in the field at Shunyi experimental site (Institute of Crop Sciences, CAAS, 40º13′52″ N, 116º33′52″ E). Planting occurred in late February, and harvesting for yield analysis occurred in July. For drought treatment conditions, no supplementary irrigation was carried out from sowing to harvest, whereas the control group received irrigation at the jointing and grain-fill stages.

Determination of Malondialdehyde (MDA) content, Proline (PRO) content, and Catalase (CAT) activity

Physiological indicators (MDA content, PRO content, and CAT activity) were quantified using commercial assay kits from Suzhou Comin Biotechnology Co., Ltd. (Suzhou, China). Measurements were performed in 96-well plates according to the manufacturer's protocols for tissue sample extraction and detection, with absorbance readings obtained via a microplate reader. Take 0.05 g of treated plant leaves, grind them in liquid nitrogen, and proceed with physiological index analysis. The results were calculated based on sample mass according to the specified formula in the corresponding manuals (MDA: https://www.cominbio.com/uploads/soft/190325/2-1Z325154356.pdf; PRO content: https://www.cominbio.com/uploads/soft/180727/1-1PHGF414.pdf; CAT activity: https://www.cominbio.com/uploads/soft/210330/1-210330161952.pdf).

For the drought treatment experiment, physiological parameters were assessed five days after rewatering. In the experiment examining the impact of FCR on drought resistance, the samples were collected five days after *Fpg* infection. To ensure the wheat stem base was sufficiently thick for inoculation with *Fpg* spore suspension at the onset of drought symptoms, an additional 100 ml of water was applied to each pot during the seedling stage, in accordance with the initial soil moisture requirements of the drought treatment.

Preparation of plant extracts and evaluation of their inhibitory effects on *Fpg* growth

Grind 25 g of stem tissue from transgenic and WT lines into a powder, and add it to 200 mL of 95% ethanol. Shake the mixture at 200 rpm/min for 12 hours at 4°C. Centrifuge at 13,500 g for

15 min and collect the supernatant. Repeat the extraction steps with the solid residue, and combine the twice supernatants. Concentrate the filtrate to 20mL using a rotary evaporator and adjust the concentration to 1g/ml[49,50]. The extracts were added to PDA solid medium and CMC liquid medium to investigate the effects on the growth of *Fpg*.

RNA extraction, transcriptome sequencing and enrichment analyses

One cm seedlings of PBZ300 germinated on damp filter paper were transferred to a sterile cultivation basin. The *Fpg* spore suspensions were inoculated 15 days later. Stem segments (2 cm in length) located immediately above the point of contact with the diseased wheat kernels were excised at 0, 2, and 4 days post-inoculation. For each biological replicate, stem base tissues from five individual plants were pooled. Total RNA for transcriptome analysis was extracted using an RNA Easy Fast Plant Tissue Kit (TianGen, Beijing). Transcriptome sequencing was performed by MetWare Biotechnology Co., Ltd. (Wuhan), which also constructed the transcriptome library and carried out the sequencing on an Illumina HiSeq platform. Transcriptome analysis of the *TaMPK3*-transformed lines was performed using stem base tissues collected from plants grown under normal conditions for 20 days. Sampling and sequencing procedures followed the same methods as described above.

Transcriptome sequencing following drought treatment was performed on Fielder grown under different water conditions when the leaves showed drooping symptoms indicative of water deprivation. Leaf tissues were collected from both drought-treated and control groups. RNA-seq was conducted by TianGen. Fastp v0.19.3 software was used to filter the original data and remove adapters from the reads. Paired-end reads were aligned to the Chinese Spring IWGSC RefSeq 1.0 reference genome by the HISAT2 procedure, and read counts mapped to each gene were quantified using HTSeq v.0.6.1. Differentially expressed genes (DEGs) were identified by DESeq2 with the thresholds $\log^2$ (FoldChange) > 1 and FDR < 0.05. GO and KEGG enrichment analyses of DEGs were performed with functional annotation tool in DAVID (Database for Annotation, Visualization, and Integrated Discovery) database (https://davidbioinformatics.nih.gov/). The results of enrichment analyses were visualized using the clusterProfiler package in R.

RT-qPCR analysis

First-strand cDNA for RT-qPCR analysis was synthesized from total RNA extracted from the stem bases of plants subjected to drought treatment and *Fpg* infection, using the FastKing RT Kit with gDNase (TianGen). RT-qPCR was performed on a TGreat Real qPCR system (OSE-R96) using Talent qPCR PreMix (SYBR Green), according to the manufacturer's protocol. Expression levels were determined using the 2^(-ΔΔCT) method. All RT-qPCR primers are listed in Supplementary Data 1.

Extraction of total plant protein and analysis of protein abundance

For total protein extraction, grind 100 mg of plant tissue into powder in liquid nitrogen, add 500 µl NB1 buffer[37], and collect the supernatant after two centrifugation steps (13,500 g, 10 min, 4°C). The protein abundance of TaMPK3 and TaCYP51H37-flag were determined with p44/42 MAPK(Erk1/2) Rabbit mAb (CST, 4695S) and Flag-Tag Mouse mAb (YEASEN, 30503ES20) at a 1:4000 dilution though immunoblot methods.

Stem base inoculation and *Fpg* mycelia staining

Collect the 3.5 cm stem base tissues from transgenic and WT lines. At 0.5 cm intervals along the stem base, create a puncture wound with an injection needle (0.45 mm). Submerge the wounded area in *Fpg* spore suspensions for 12 hours. Then, culture the stem on moist filter paper in a shaded environment for three days and assess the changes in the wound.

For Trypan Blue staining**,** excise the outermost layer of stem tissue surrounding the wound. Subsequently, incubate the sample in a decolorization solution (10% KOH) at 40°C for 3 h, stain it with 0.05% Trypan Blue dye for 3 h. Rinsed the sample five times with 0.1 M Tris–HCl buffer (pH 8.0), and then observe the mycelia under a microscope.

For Wheat Germ Agglutinin (WGA) staining**,** basal tissue from healthy wheat stems was immersed in spore suspensions for 6 h and subsequently cultured on moist filter paper for three days. The outermost layer of the stem tissue was peeled off and incubated in 1 M KOH at 37°C for 24 h in darkness. The stems were rinsed three times with 50 mM Tris–HCl (pH 7.4) and stained with WGA at a concentration of 20 µg/mL in the Tris–HCl buffer under dark condition at 4°C for

24 h. The samples were then observed with a Zeiss LSM700 microscope.

Virus-induced gene silencing (VIGS) and assessment of FCR severity

The 400-450 bp fragments of the *TaCYP51H37*, *TaWRKY26*, *TaHSD*, *TaCYP51H35* and *TaOSC* genes were analyzed for potential off-target genes (Supplementary Figure 34) and cloned into the γ vector of the VIGS system, all primers used for cloning target fragments are listed in Supplementary Data 1. The α vector, β vectors, along with the recombinant γ vector and the control empty γ vector were individually transcribed into RNAs. These RNAs were mixed in different combinations and used to infect wheat seedlings at the three-leaf stage according to the BSMV-VIGS protocol[51]. Eight days after virus infection, three new leaves per pot were collected and pooled to extract RNA. The expression of the target gene was then determined using the RT-PCR. *Fpg* spores were injected into VIGS-silenced and control plants, and the growth status and disease indices were assessed 14 days later.

Construction of co-expression networks and identification of co-expressed transcription factor genes involved in regulating of sterol synthesis genes

Transcriptome data of *Fpg*-infected wheat variety PuBingZi300 (0 d, 2 d and 4 d) and Jimai22 (0 d, 3 d and 11 d), along with 14 wheat tissue expression data (radicle, root-seeding, root-mature, coleoptile, shoot-apical-meristem, stem, internode, first-leaf-sheath, first -leaf-blade, flag-leaf-sheath, flag-leaf-blade, peduncle, spike, spikelet) obtained from the wheat-URGI website (https://wheat-urgi.versailles.inrae.fr/), were used for construct co-expression networks. A weighted gene co-expression network analysis (WGCNA) was conducted using the WGCNA program in Metware Cloud platform (https://cloud.metware.cn/). Based on the WGCNA results, co-expressed transcription factors associated with sterol synthesis genes were identified, with a weight value threshold set at ≥0.1. Additionally, the co-expression database for multiple wheat tissues on the WheatOmics 1.0 website (http://202.194.139.32/) was also used to confirm the results of the WGCNA analysis. In this database, a Pearson correlation coefficient (PCC) threshold of ≥0.6 was applied. The results were visualized using Cytoscape software.

Yeast hybrid assays

The coding sequence of *TaMPK3* for yeast two-hybrid (Y2H) assays was cloned into the pGBKT7 vector, and full-length sequences of transcription factors were cloned into the pGADT7 vector. Y2H assays were performed using the yeast strain AH109 (Coolaber) according to the manufacturer's protocol. To identify the TaWRKY26 transcription factor that binds to the promoters of sterol synthesis genes, a 400-600 bp promoter sequence was cloned into the pHIS2 vector, and the yeast one-hybrid (Y1H) assays were performed using the yeast strain Y187 (Coolaber) according to the manufacturer's protocol. All primers used for cloning target gene and promoter sequence are listed in Supplementary Data 1.

Bimolecular fluorescence complementation (BIFC) and luciferase complementation imaging (LCI) assays

For BIFC assays, the *TaMPK3* gene was cloned into the pXY104 vector containing the cYFP sequence, and the TaWRKY transcription factor was cloned into the pXY106 vector containing the nYFP sequence. The pXY104-TaMPK3 and pXY106-TaWRKY vectors were introduced into the *Agrobacterium* strain GV3101 and then used to infect tobacco leaves in different combinations. After injection, the tobacco plants were kept in the dark for one day and then grown under light for an additional day. The YFP fluorescence in the tobacco leaves was imaged using an LSM700 microscope.

For LCI assays, the *TaMPK3* and *TaWRKY* genes were cloned into the pCAMBIA1300-nLUC and pCAMBIA1300-cLUC vectors, respectively. Tobacco plants was treated according to the BIFC experimental method, and the leaves were treated with D-luciferin. Luciferase activity was measured using a low-light cooled Charge-Coupled Device (CCD) imaging apparatus (Night SHADE LB 985). All primers used for cloning target gene are listed in Supplementary Data 1.

Dual-luciferase reporter assays

To determine transcriptional activity, the *TaMPK3* and *TaWRKY26* genes were cloned into pCAMBIA2300, and 400-600 bp promoters of sterol synthesis genes were cloned into the pGreen0800II vector. The recombinant and control vectors were introduced into GV3101 and used

in different combinations to infect tobacco leaves and wheat protoplasts. Subsequent experimental methods on tobacco leaves were similar to those used in LCI assays. Co-transformation into wheat leaf protoplasts was performed using PEG-mediated transformation methods. Then the protoplasts were incubated at 23°C for 16 h. Total protein was extracted using a Plant Total Protein Extraction Kit (CoWin Biosciences, Boston, MA. USA), and detected using the dual-LUC Reporter Assay System (Promega, Madison, WI, USA). LUC data were collected using an automatic microplate reader. All primers used for cloning target gene and promoter sequence are listed in Supplementary Data 1.

Pull-down and phosphorylation assays *in vitro*

The *TaMPK3* gene was cloned into the pMAL-5 vector containing the maltose-binding protein (MBP) sequence, and the *TaWRKY* genes was cloned into the pCold vector containing the His-Tag sequence. All primers used for cloning target gene are listed in Supplementary Data 1. Recombinant fusion proteins TaMPK3-MBP and TaWRKY-His were expressed in Transetta (DE3) cells (TransGen, Beijing) and purified with Amylose Resin (E8021S; NEB, Ipswich, MA, USA) and Ni-NTA Resin (DP101-01; TransGen), respectively. TaMPK3-MBP proteins, TaWRKY-His proteins and His Resin were co-incubated overnight at 4°C with constant rotation in 300 µl of pull-down buffer (40 mM HEPES, 10 mM KCl, 0.4 M sucrose, 3 mM MgCl2, 1 mM EDTA, 1 mM dithiothreitol, 0.2% Triton X-100). The retained His Resin was washed five times with 1 ml of 1× phosphate-buffered saline (PBS) and analyzed using an anti-MBP antibody (TransGen, HT701-01) at a 1:4000 dilution.

For autophosphorylation of TaMPK3, 1 µg of TaMPK3-MBP protein was incubated in 50 µl of reaction buffer (20 mM HEPES, 10 mM $MgCl_2$, 1 mM DTT, and 25 µM ATP) for 1 h at 25°C. The reaction was terminated by adding SDS loading buffer and analyzed using a 75 µM Phos-Tag™ Acrylamide AAL-107 assay (F4002; APExBIO, Houston, TX, USA) with an anti-MBP monoclonal antibody. For TaMPK3-mediated phosphorylation, 2 µg of TaMPK3-GST was incubated with 1 µg of TaWRKY-His in 50 µl reaction buffer. The subsequent experimental procedures were conducted following the autophosphorylation assay procedures and were detected

using an anti-His antibody (TransGen, HT501-01) at a 1:4000 dilution.

***In vitro* electrophoretic mobility shift assays (EMSA)**

Biotin-labeled probes targeting sterol synthesis genes were synthesized by AuGCT (China); the sequences are provided in Supplementary Data 2. Oligonucleotides were heated at 95°C for 10 min and subsequently cooled to room temperature to form double-stranded DNA. EMSA was performed using a LightShift Chemiluminescent EMSA Kit (Thermo Fisher, USA). Biotin-labeled probes were incubated with 2 μg of purified TaWRKY26-His fusion protein at 25°C for 30 mins. The DNA-protein complexes was separated using a 6% polyacrylamide gel and transferred to nylon membranes (Millipore, USA). Signals were detected using an EasySee Western Blot Kit according to the manufacturer's instructions.

Data availability

Data supporting the findings of this work are available within the paper and its supplementary information files. The raw RNA-seq reads from wheat inoculated with *Fpg* have been deposited in the NCBI Database (https://www.ncbi.nlm.nih.gov/sra) under Sequence Read Archive (SRA) BioProject ID: PRJNA1139870. The SRA data from the transcriptome analysis of the *TaMPK3*-transformed line and WT have been submitted under BioProject PRJNA1276293. The SRA data for wheat under drought treatment are available under BioProject ID: PRJNA1056048. The SRA data for *Fpg*-infected wheat variety Jimai22 are stored under BioProject ID: PRJNA1390310. Source data are deposited in Figshare (https://doi.org/10.6084/m9.figshare.29586923).

References

1. Desmond, O. J., Manners, J. M., Schenk, P. M., Maclean, D. J. and Kazan, K. Gene expression analysis of the wheat response to infection by *Fusarium pseudograminearum*. *Physiol Mol Plant. P* **73,** 40-47 (2008).

2. Murray, G. M. and Brennan, J. P. Estimating disease losses to the Australian wheat industry. *Australas Plant Path*. **38,** 558-570 (2009).

3. Smiley, R. W., Gourlie, J. A., Easley, S. A. and Patterson, L. M. Pathogenicity of *Fungi* associated with the wheat crown rot complex in Oregon and Washington. *Plant Dis*. **89,** 949-957 (2005).

4. Mishra, P. K., Tewari, J. P., Clear, R. M. and Turkington, T. K. Genetic diversity and recombination within populations of *Fusarium pseudograminearum* from western Canada. *Int Microbiol*. **9,** 65-8 (2006).

5. Kazan, K. and Gardiner, D. M. *Fusarium* crown rot caused by *Fusarium pseudograminearum* in cereal crops: recent progress and future prospects. *Mol Plant Pathol*. **19,** 1547-1562 (2018).

6. Beccari, G. et al. Development of three *Fusarium* crown rot causal agents and systemic translocation of deoxynivalenol following stem base infection of soft wheat. *Plant Pathol*. **67,** 1055–1065 (2018).

7. Ma, G. et al. Isolation, characterization, and pathogenicity of *Fusarium* species causing crown rot of wheat. *Front Microbiol*. **30,** 1405115 (2024).

8. Summerell, B. A. and Burgess, L. W. Stubble management practices and the survival of *Fusarium graminearum* Group 1 in wheat stubble residues. *Plant Pathol*. **17,** 88-93 (1988).

9. Summerell, B. A., Burgess, L. W. and Klein, T. A. The impact of stubble management on the incidence of crown rot of wheat. *Aust J Exp Agr*. **29,** 863-867 (1989).

10. Summerell, B. A., Burgess, L. W., Klein, T. A. and Pattison, A. B. Stubble management and the site of infection of wheat by *Fusarium graminearum* Group 1. *Phytopathology*. **80,** 877-879 (1990).

11. Akinsanmi, O. A., Mitter, V., Simpfendorfer, S., Backhouse, D. and Chakraborty, S. Identity and pathogenicity of *Fusarium spp.* isolated from wheat fields in Queensland and northern New South Wales. *Aust. J. Agric. Res*. **55,** 97-107 (2004).

12. Akinsanmi, O. A., Backhouse, D., Simpfendorfer, S. and Chakraborty, S. Genetic diversity of Australian *Fusarium graminearum* and *F. pseudograminearum*. *Plant Pathol*. **55,** 494-504 (2006).

13. Chakraborty, S. et al. Pathogen population structure and epidemiology are keys to wheat crown rot and *Fusarium* head blight management. *Plant Pathol*. **36,** 643-655 (2006).

14. Tunali, B. et al. Root and crown rot fungi associated with spring, facultative, and winter wheat in Turkey. *Plant Dis*. **92,** 1299-1306 (2008).

15. Tunali, B., Obanor, F., Erginbas, G., Westecott, R. A., Nicol, J. and Chakraborty, S. Fitness of three *Fusarium* pathogens of wheat. *FEMS Microbiol Ecol*. **81,** 596-609 (2012).

16. Cook, R. J. Management of wheat and barley root diseases in modern farming systems. *Plant Pathol*. **30,** 119-206 (2001).

17. Collard, B. C. Y. et al. Development of molecular markers for crown rot resistance in wheat: mapping of QTL for seedling resistance in a '2-49' × 'Janz' population. *Plant Breed*. **124,** 532-537 (2005).

18. Collard, B. C. Y., Jolley, R., Bovill, W. D., Grams, R. A., Wildermuth, G. G. and Sutherland, M. W. Confirmation of QTL mapping and marker validation for partial seedling resistance to crown rot in wheat line '2-49'. *Aust. J. Agric. Res*. **57,** 967-973 (2006).

19. Martin, A. et al. Markers for seedling and adult plant crown rot resistance in four partially resistant bread wheat sources. *Theor Appl Genet*. **128,** 377-385 (2015).

20. Liu, C. and Ogbonnaya, F. C. Resistance to *Fusarium* crown rot in wheat and barley: a review. *Plant Breed*. **134,** 365-372 (2015).

21. Yang, X. et al. Investigation and genome-wide association study for *Fusarium* crown rot resistance in Chinese common wheat. *BMC Plant Biol*. **19,** 153 (2019).

22. Jin, J. et al. Identification of a novel genomic region associated with resistance to *Fusarium* crown rot in wheat. *Theor Appl Genet*. **133,** 2063–2073 (2020).

23. Hou, S. et al. Genome-wide association analysis of *Fusarium* crown rot resistance in Chinese wheat landraces. *Theor Appl Genet*. **136,** 101 (2023).

24. Li, J. et al. Dissecting the genetic basis of *Fusarium* crown rot resistance in wheat by genome wide association study. *Theor Appl Genet*. **137,** 43 (2024).

25. Su, Y. et al. Identification of genetic loci and candidate genes underlying *Fusarium* crown rot resistance in wheat. *Theor Appl Genet*. **138,** 23 (2025).

26. Yang, X., Zhong, S., Zhang, Q., Ren, Y., Sun, C. and Chen, F. A loss-of-function of the dirigent gene *TaDIR-B1* improves resistance to *Fusarium* crown rot in wheat. *Plant Biotechnol J*. **19,** 866-868 (2021).

27. Lv, G. et al. A cell wall invertase modulates resistance to *Fusarium* crown rot and sharp eyespot in common wheat. *J Integr Plant Biol*. **65,** 1814-1825 (2023).

28. Qi, H. et al. *TaRLK-6A* promotes *Fusarium* crown rot resistance in wheat. *J Integr Plant Biol*. **66,** 12-16 (2024).

29. Xu, X. et al. *TaWRKY24* integrates the tryptophan metabolism pathways to participate in defense against *Fusarium* crown rot in wheat. *Plant J*. **120,** 1764-1785 (2024).

30. Yang, X. et al. A TaSnRK1α-TaCAT2 model mediates resistance to *Fusarium* crown rot by scavenging ROS in common wheat. *Nat Commun*. **15;16,** 2549 (2025).

31. Zhang, N. et al. TaHSP18.6 and TaSRT1 interact to confer resistance to *Fusarium* crown rot by regulating the auxin content in common wheat. *Proc Natl Acad Sci U S A*. **15;122,** e2500029122 (2025).

32. Liu, X. and Liu, C. Effects of Drought-Stress on *Fusarium* Crown Rot Development in Barley. *Plos One*. **11,** e0167304 (2016).

33. Su, Z., Powell, J. J., Gao, S., Zhou, M. and Liu, C. Comparing transcriptional responses to *Fusarium* crown rot in wheat and barley identified an important relationship between disease resistance and drought tolerance. *BMC Plant Biol*. **21,** 73 (2021).

34. Buster, M., Simpfendorfer, S., Guppy, C., Sissons, M. and Flavel, R. J. *Fusarium* crown rot reduces water use and causes yield penalties in wheat under adequate and above average water availability. *Agronomy*. **12,** 2616 (2022).

35. Su, Z. et al. Transcriptomic insights into shared responses to *Fusarium* crown rot infection and drought stresses in bread wheat (*Triticum aestivum L.*). *Theor Appl Genet*. **137,** 34 (2024).

36. Polturak, G., Dippe, M., Stephenson, M. J. and Osbourn, A. Pathogen-induced biosynthetic pathways encode defense-related molecules in bread wheat. *Proc Natl Acad Sci U S A*. **119,** e2123299119 (2022).

37. Liu, Y. et al. Mitogen-activated protein kinase TaMPK3 suppresses ABA response by destabilising TaPYL4 receptor in wheat. *New Phytol*. **236,** 114-131 (2022).

38 Mao, H. et al. The wheat ABA receptor gene *TaPYL1-1B* contributes to drought tolerance and grain yield by increasing water-use efficiency. *Plant Biotechnol J*. **20,** 846-861 (2022).

39 Zhang, Y. et al. Wheat TaPYL9-involved signalling pathway impacts plant drought response through regulating distinct osmotic stress-associated physiological indices. *Plant Biotechnol J*. **23,** 352-373 (2025).

40 Wang, Q. et al. Abscisic acid-, stress-, ripening-induced 2 like protein, TaASR2L, promotes wheat resistance to stripe rust. *Mol Plant Pathol*. **25,** e70028 (2024).

41 Sun, T. and Zhang, Y. MAP kinase cascades in plant development and immune signaling. *EMBO Rep*. **23,** e53817 (2022).

42 Hao, L., Wen, Y., Zhao, Y., Lu, W. and Xiao, K. Wheat mitogen-activated protein kinase gene TaMPK4 improves plant tolerance to multiple stresses through modifying root growth, ROS metabolism, and nutrient acquisitions. *Plant Cell Rep*. **34,** 2081-97 (2015).

43 Shu, W. et al. Wheat MAPK cascade mediates SGT1 nuclear entry targeted by a stripe rust effector. *J Integr Plant Biol*. **67,** 1614-1632 (2025).

44 Su, J. et al. Active photosynthetic inhibition mediated by MPK3/MPK6 is critical to effector-triggered immunity. *PLoS Biol*. **16,** e2004122 (2018).

45 Kim, S. H. et al. Phosphorylation of the auxin signaling transcriptional repressor IAA15 by MPKs is required for the suppression of root development under drought stress in *Arabidopsis*. *Nucleic Acids Res*. **50,** 10544-10561(2022).

46 Yu, T. F. et al. Soybean steroids improve crop abiotic stress tolerance and increase yield. *Plant Biotechnol J*. **22,** 2333-2347 (2024).

47 Chen, M. et al. Cholesterol accumulation by suppression of SMT1 leads to dwarfism and improved drought tolerance in herbaceous plants. *Plant Cell Environ*. **41,** 1417-1426 (2018).

48. Li, X., Liu, C., Chakraborty, S., Manners, J. M. and Kazan, K. A simple method for the assessment of crown rot disease severity in wheat seedlings inoculated with *Fusarium pseudograminearum*. *J Phytopathol*. **1986,** 751-754 (2008).

49. Redfern, J., Kinninmonth, M., Burdass, D. and Verran, J. Using soxhlet ethanol extraction to produce and test plant material (essential oils) for their antimicrobial properties. *J Microbiol Biol Edu*. **15,** 45-6 (2014).

50. Chen, X. et al. Analysis of triterpene chemical constituents in poria cocos 95% ethanol extract via UPLC-IT-TOF/MS. *J K M MED UNIV*. **42,** 1-8 (2021).

51. Holzberg, S., Brosio, P., Gross, C. and Pogue, G. P. Barley stripe mosaic virus-induced gene silencing in a monocot plant. *Plant J*. **30,** 315-27 (2002).

Acknowledgements

This work was supported by the National Key R&D Program of China (2022YFF1001600), the National Natural Science Foundation of China (32472197 and 32572317), the Major Project on Agricultural Bio-breeding of China (2023ZD04026), Basic Research Center, Innovation Program of Chinese Academy of Agricultural Sciences (CAAS-CSNCB-202302), Central Public-interest Scientific Institution Basal Research Fund (S2026QZ17), the inner Mongolia Natural Science Foundation (2024QN03037). We are grateful to Dr Lihui Li, Institute of Crop Science Chinese Academy of Agricultural Sciences (CAAS), Academician Weigang Xu, Triticeae Research Institute, Henan Academy of Agricultural Sciences, Academician Zhensheng Kang, College of Plant Protection, Northwest A&F University, Robert A. McIntosh, the University of Sydney, and Dr S Mayes, CIMMYT, for kindly providing wheat seeds and helpful reviews.

Author Contributions

Z.S.X coordinated the project, conceived and designed experiments; L.Z, T.F.Y, Y.L and Z.H.H performed most of the experiments and analyzed the data; L.Z wrote the article; Y.Z.M, L.H.L, M.C, Y.B.Z, X.L.Z, J.C, X.Y.C, Y.W.L, J.N.R, G.Y.C, S.X.Z and X.F.M commented and edited the manuscript; L.H.L provided wheat seeds; W.Z.H, J.M.H, J.T.W, X.X, X.R.W, W.W, J.P.Z, Y.F.J and X.Y.L investigated traits and assisted in experiments. All authors have read and approved the final manuscript.

Competing interests

The authors declare no competing interests

Figure 1. Effects of drought on FCR symptoms and transcriptomic analyses under drought stress and *Fpg* infection.

(a) Illustration of stem surface infection using *Fpg* infected wheat kernels. Created in BioRender. Su, F. (2026) https://BioRender.com/immdf66. (b, c) Disease symptoms and indices following

stem surface infection under drought and normal conditions; n = 36 biologically independent plants. (d) Illustration of stem internal injection using *Fpg* spore suspensions. Created in BioRender. Su, F. (2026) https://BioRender.com/immdf66. (e, f) Disease symptoms and indices following stem internal injection; n = 36 biologically independent plants. (g) Venn diagrams were used to depict the DEGs under *Fpg*-infected and drought treatments. (h) KEGG enrichment analysis of 762 DEGs that were up-regulated under *Fpg* infection and down-regulated in response to drought treatment. (i) The enrichment condition of DEGs in the MAPK signaling pathway, the enriched DEGs were highlighted in red. (j) Transcriptome data of DEGs within the MAPK signaling pathway. (k-m) Expression analyses of homologous *TaMPK3* genes in stem bases under drought stress and *Fpg* infection. Statistical significance was determined by a two-tailed Student's t test (***P<0.001).

Figure 2. Generation of *TaMPK3* gene overexpression and gene-edited lines, and identification of FCR resistance in transgenic and WT plants.

(a) Mutation sites in gene-edited lines. (b) The growth status of transgenic lines and WT under normal conditions and during *Fpg* infection; bars, 10 cm. The OE represents gene overexpression lines and KO (Knockout) represents the gene-edited lines. (c) Disease symptoms of transgenic lines and WT under *Fpg* infection; bar, 5 cm. (d) The expression of the *TaMPK3* genes was detected in transgenic plants and WT plants. In box plots, the line represents the median, the edges of the box define the interquartile range, and the whiskers represent the minimum and maximum values. (e) The statistics of disease indices in transgenic lines and WT plants; n = 18 biologically independent plants per line. (f-h) The shoot length, fresh weight and dry weight were measured under normal conditions and during *Fpg* infection; n = 15 biologically independent plants per line. Statistical significance was determined by a two-tailed Student's t test (*p < 0.05, **p < 0.01, ***p < 0.001). If pairwise comparisons of each of the three lines against the control yield P-values < 0.001, the figure reports the overall P-value obtained from a combined statistical test comparing the pooled experimental group (i.e., all three lines) with the control group.

Figure 3. Identification of drought tolerance and yield traits in transgenic and WT plants.

(a) The growth statuses of seedlings from transgenic lines and WT plants cultivated under water-deficit and rehydration conditions; bars, 10 cm. (b-e) Dry weight, CAT activity, MDA and PRO contents were detected in transgenic lines and WT plants; n = 12 biologically independent plants per line were used for dry weight analysis, n = 5 biologically independent plants per line were used for CAT activity, MDA and PRO contents analysis. (f) The growth statuses of transgenic lines and WT plants under normal and drought conditions in the field; bars, 20 cm. (g-k) The growth and yield traits of transgenic lines and WT plants grown in the field; n = 12 biologically independent plants per line were used for plant height, panicle length and effective spike number analysis, n = 19 biologically independent plants per line were used for grain weight per plant and thousand grain weight analysis. In box plots, the line represents the median, the edges of the box define the interquartile range, and the whiskers represent the minimum and maximum values. Statistical significance was determined by a two-tailed Student's t test (***p < 0.001). If pairwise comparisons of each of the three lines against the control yield P-values < 0.001, the figure reports the overall P-value obtained from a combined statistical test comparing the pooled experimental group (i.e., all three lines) with the control group.

Figure 4. The effects of the *TaMPK3* gene on the growth suppression of *Fpg* in wheat.

(a) The wound sites on the stem bases of *TaMPK3*-OE, WT and *TaMPK3*-KO lines were inoculated with *Fpg* spore suspensions; bars, 1 cm. (b) The trypan blue staining of the mycelia at the wound sites; bars, 0.5 mm. (c) The WGA fluorescence staining of the mycelia. (d) The mycelia growth of *Fpg* on the PDA medium containing 0.8 and 1.6 mg/mL extracts from transgenic lines and WT plants; bars, 2 cm. (e) The mycelial diameter of *Fpg* was calculated; n = 3 biologically independent colony per line. Data are presented as mean values +/- SD. If pairwise comparisons of each of the three lines against the control yield P-values < 0.001, the figure reports the overall P-value obtained from a combined statistical test comparing the pooled experimental group (i.e., all three lines) with the control group. (f) The growth statuses of *Fpg* growth in CMC medium containing 30 and 60 mg/mL extracts; bars, 0.1 mm. (g) The absorbance of *Fpg* solutions was measured in the presence of extracts at different concentrations; n = 3 biologically independent *Fpg* solutions per line.

Statistical significance was determined by a two-tailed Student's t test (*p < 0.05, **p < 0.01, ***p < 0.001).

Figure 5. Transcriptome analysis identifies genes and pathways influenced by the *TaMPK3* gene and *Fpg* infection.

(a) The Venn diagram illustrated 366 DEGs that are regulated by the *TaMPK3* gene and are up-regulated upon *Fpg* infection. (b-c) The GO and KEGG enrichment analyses of 366 DEGs. BP, biological process; MF, molecular function. (d) Transcriptome data of sterol synthesis genes. (e) Distribution of the identified sterol synthesis genes on chromosomes 5A and 5D. (f) The sterol synthesis genes involved in ellarinacin synthesis. (g-q) Expression levels of sterol synthesis genes were measured in the stem bases of transgenic lines and WT plants. Statistical significance was determined by a two-tailed Student's t test (***p < 0.001). If pairwise comparisons of each of the three lines against the control yield P-values < 0.001, the figure reports the overall P-value obtained from a combined statistical test comparing the pooled experimental group (i.e., all three lines) with the control group.

Figure 6. Functional analysis of the sterol synthesis gene *TaCYP51H37* in relation to FCR resistance.

(a) The growth statuses of *TaCYP51H37*-OE lines and WT plants under normal conditions and upon *Fpg* infection; bars, 10 cm. (b) The expression of the *TaCYP51H37* gene was detected in transgenic lines and WT plants. (c) Disease symptoms were observed in *TaCYP51H37*-OE lines and WT plants 30 days after *Fpg* infection; bar, 5 cm. (d) The statistics of disease indices in transgenic lines and WT plants; n = 21 biologically independent plants per line. (e-g) Analyses of shoot length, fresh weight, and dry weight of *TaCYP51H37*-OE lines and WT plants; n = 15 biologically independent plants per line. (h) The browning degree of the wounds on the stem bases of infected *TaCYP51H37*-OE lines and WT plants; bars, 1 cm. (i) The trypan blue staining of mycelia at wound sites; bars, 0.5 mm. (j) The mycelia growth analysis of *Fpg* on PDA medium containing extracts from *TaCYP51H37*-OE lines and WT plants; bar 2 cm. (k) The mycelial

diameter of *Fpg* was calculated; n = 3 biologically independent colony per line. Data are presented as mean values +/- SD. If pairwise comparisons of each of the three lines against the control yield P-values < 0.001, the figure reports the overall P-value obtained from a combined statistical test comparing the pooled experimental group (i.e., all three lines) with the control group. (l) The growth statuses of *Fpg* were analyzed in CMC medium containing extracts; bars 0.1 mm. (m) The absorbance of the *Fpg* solution after treatment with various concentrations of the extracts; n = 3 biologically independent *Fpg* solutions per line. Statistical significance was determined by a two-tailed Student's t test (*p < 0.05, **p < 0.01, ***p < 0.001).

Figure 7. Screening and identification of transcription factors regulating sterol synthesis genes.

(a) Co-expression network analysis of transcription factors associated with sterol synthesis genes. (b) Interactions between transcription factors and TaMPK3 protein were detected through yeast two-hybrid assays (Y2H). (c) The BIFC assay was used to identify the interaction between TaWRKY transcription factors and TaMPK3 protein. (d) The interactions were verified via LCI assays in tobacco leaves. (e) Pull-down assay was conducted to confirm the interactions *in vitro*. The Y2H, BIFC, LCI and Pull-down assays were done independently three times with similar results.

Figure 8. The TaMPK3 protein modulates the expression of sterol synthesis genes by phosphorylating the TaWRKY26 transcription factor.

(a) The phos-tag assay was used to verify that the TaMPK3 protein phosphorylated TaWRKY transcription factors. (b) Yeast one-hybrid (Y1H) assays were conducted to confirm the interaction between TaWRKY26 protein and the promoter regions of sterol synthesis genes. (c) The EMSA demonstrated that the TaWRKY26 protein binds specifically to the promoter regions. (d) The vector constructs were used in dual-LUC reporter assays. (e) The dual-LUC reporter assays confirmed that sterol synthesis genes are regulated by the TaWRKY26 and TaMPK3 proteins in wheat protoplasts; n = 4 biologically independent samples. (f) Detection of LUC activity signals

in tobacco leaves via CCD imaging. Statistical significance was determined by a two-tailed Student's t test (**p < 0.01, ***p < 0.001). The phos-tag, Y1H, EMSA and dual-LUC reporter assays were done independently three times with similar results.

Figure 9. The synergistic effect of drought and FCR in exacerbating damage to wheat was investigated.

(a, c, e and g) The effects of *Fpg* infection on drought tolerance of WT plants and transgenic plants (*TaMPK3*-OE, *TaMPK3*-KO and *TaCYP51H37*-OE). (b, d, f and h) Analysis of dry weight, CAT activity, MDA and PRO contents was performed in both WT and transgenic plants under control conditions and following *Fpg* infection; n = 10 biologically independent plants per line were used for fresh weight analysis, n = 6 biologically independent plants per line were used for CAT activity, MDA and PRO contents analysis. (i) The FCR symptoms in *TaMPK3*-OE lines, (k) *TaMPK3*-KO lines, and (m) *TaCYP51H37*-OE lines under normal and drought conditions. (j, l and n) Analyses of FCR disease indices of transgenic lines (*TaMPK3*-OE, *TaMPK3*-KO and *TaCYP51H37*-OE); n = biologically independent plants. Data are presented as mean values +/- SD. Statistical significance was determined by a two-tailed Student's t test (*p < 0.05, **p < 0.01, ***p < 0.001). If pairwise comparisons of each of the three lines against the control yield P-values < 0.001, the figure reports the overall P-value obtained from a combined statistical test comparing the pooled experimental group (i.e., all three lines) with the control group.

Figure 10. The synergistic effect of drought and FCR is mediated through the TaMPK3 regulatory pathway.

Under normal conditions, following infection with *Fpg*, the expression of *TaMPK3* and *TaWRKY26* genes are up-regulated in response to FCR. The TaMPK3 protein phosphorylates TaWRKY26, thereby enhancing FCR resistance by regulating the expression of downstream sterol synthesis genes. However, when *TaMPK3* expression increases, more TaMPK3 protein binds to the ABA receptor protein TaPYL4, promoting its degradation. Consequently, the drought tolerance of wheat is reduced, resulting in more severe damage under drought stress. Under drought

conditions, plants respond to drought signals, suppressing the expression of *TaMPK3* and *TaWRKY26* genes. The released TaPYL4 protein then binds to the PP2C protein, which releases SnRK2 (SNF1-regulated protein kinase 2s) and activats the ABA signaling pathway to enhance stress resistance. However, this process weakens resistance to FCR, exacerbating FCR severity under drought. Through this mutual reinforcement, the detrimental effects on wheat progressively intensified. Created in BioRender. Su, F. (2026) https://BioRender.com/k99x84u.

Editor's Summary

This study shows that the TaMPK3 signaling pathway regulates wheat resistance to *Fusarium* crown rot (FCR) and reveals TaMPK3-mediated synergistic damage from FCR and drought, thereby providing a mechanistic basis for drought-aggravated FCR severity.

Peer review information: *Nature Communications* thanks Zhiyong Liu, Weihua Tang and the other anonymous reviewer(s) for their contribution to the peer review of this work. A peer review file is available.

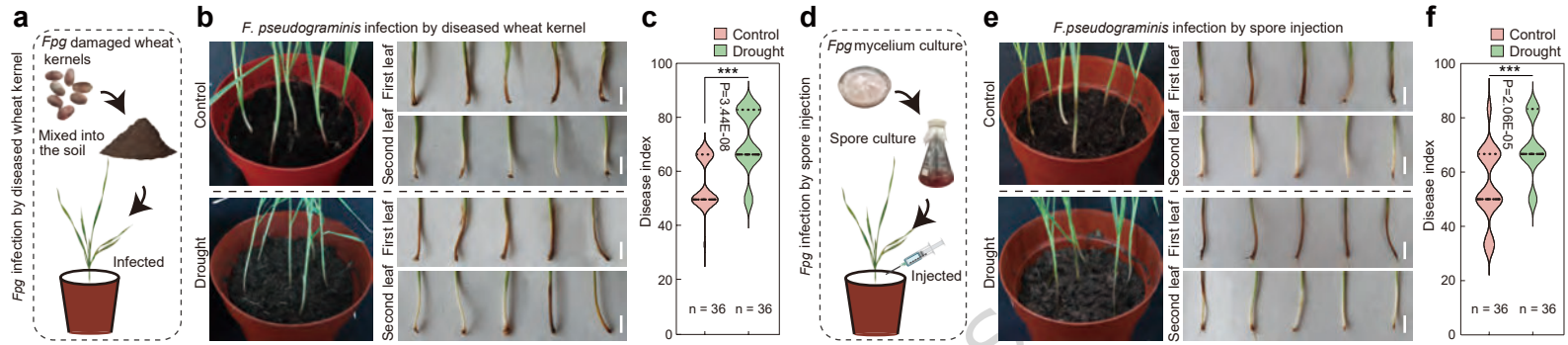

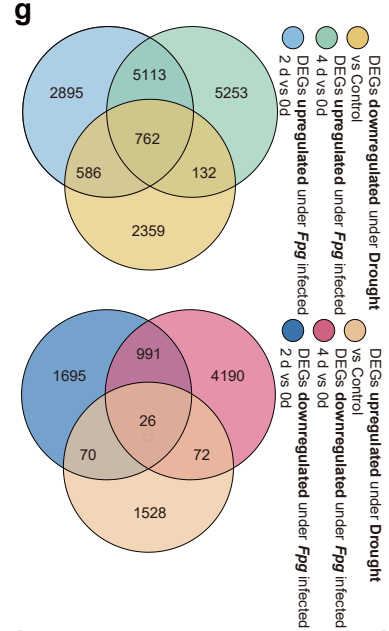

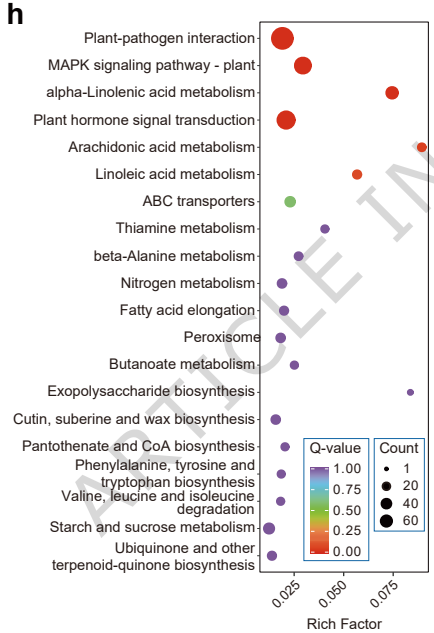

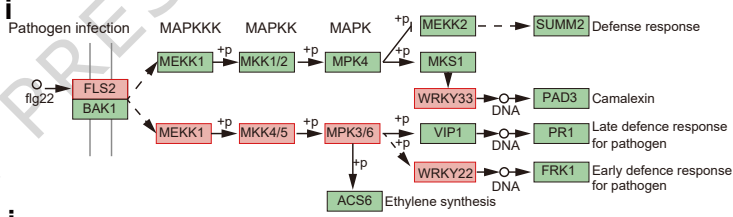

j

	Gene ID	FPKM					Description
		0 d	2 d	4 d	Control	Drought	
FLS2	TraesCS2D02G462000	0.16	7.61	0.52	0.36	0.02	LRR receptor-like serine/threonine-protein kinase FLS2
	TraesCS2A02G461800	0.87	7.95	2.22	0.39	0.04	LRR receptor-like serine/threonine-protein kinase FLS2
MEKK	TraesCS3D02G256600	0.26	20.15	2.65	12.55	1.25	Mitogen-activated protein kinase kinase kinase17
	TraesCS1D02G372400	0.00	5.25	0.71	0.90	0.26	Mitogen-activated protein kinase kinase kinase17
MKK4/5	TraesCS6D02G328800	3.25	20.64	12.57	4.09	2.68	Mitogen-activated protein kinase kinase 4
	TraesCS4B02G239400	1.04	9.80	3.70	17.80	5.05	Mitogen-activated protein kinase kinase 9
	TraesCS4D02G239400	1.29	13.07	7.04	16.55	9.64	Mitogen-activated protein kinase kinase 9
MPK3/6	TraesCS4B02G197800	2.38	128.90	43.06	51.06	24.44	Mitogen-activated protein kinase 3
	TraesCS4A02G106400	2.07	72.26	23.49	22.21	12.63	Mitogen-activated protein kinase 3
	TraesCS4D02G198600	1.58	86.86	26.99	41.96	22.63	Mitogen-activated protein kinase 3
WRKY	TraesCS1B02G088900	0.06	2.82	1.95	46.44	17.34	WRKY transcription factor 26
	TraesCS1A02G070400	1.45	99.37	54.45	35.57	15.35	WRKY transcription factor 26
	TraesCS1D02G072900	2.03	128.28	64.87	52.16	25.42	WRKY transcription factor 26
	TraesCS3A02G229300	0.14	3.20	1.18	1.81	0.68	WRKY transcription factor 22
	TraesCS3B02G255400	0.16	3.60	1.32	1.73	0.27	WRKY transcription factor 22
	TraesCS3D02G227400	0.24	4.81	1.44	2.44	0.97	WRKY transcription factor 22

FPKM: 50.00, 40.00, 30.00, 20.00, 10.00, 0.00

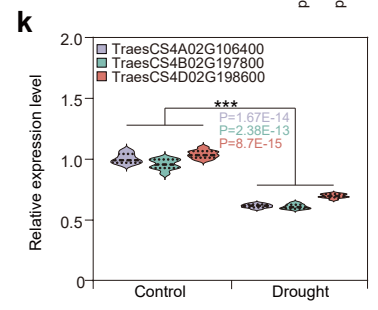

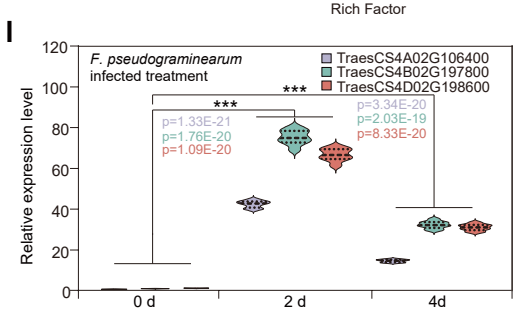

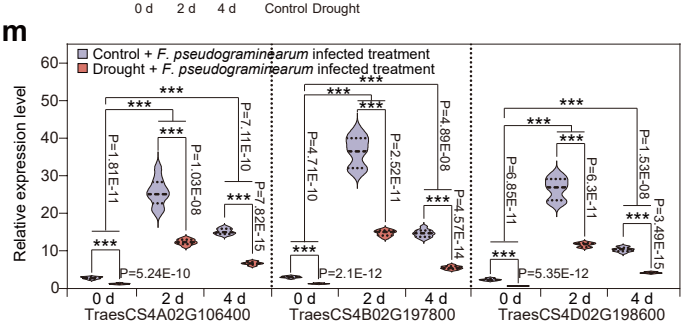

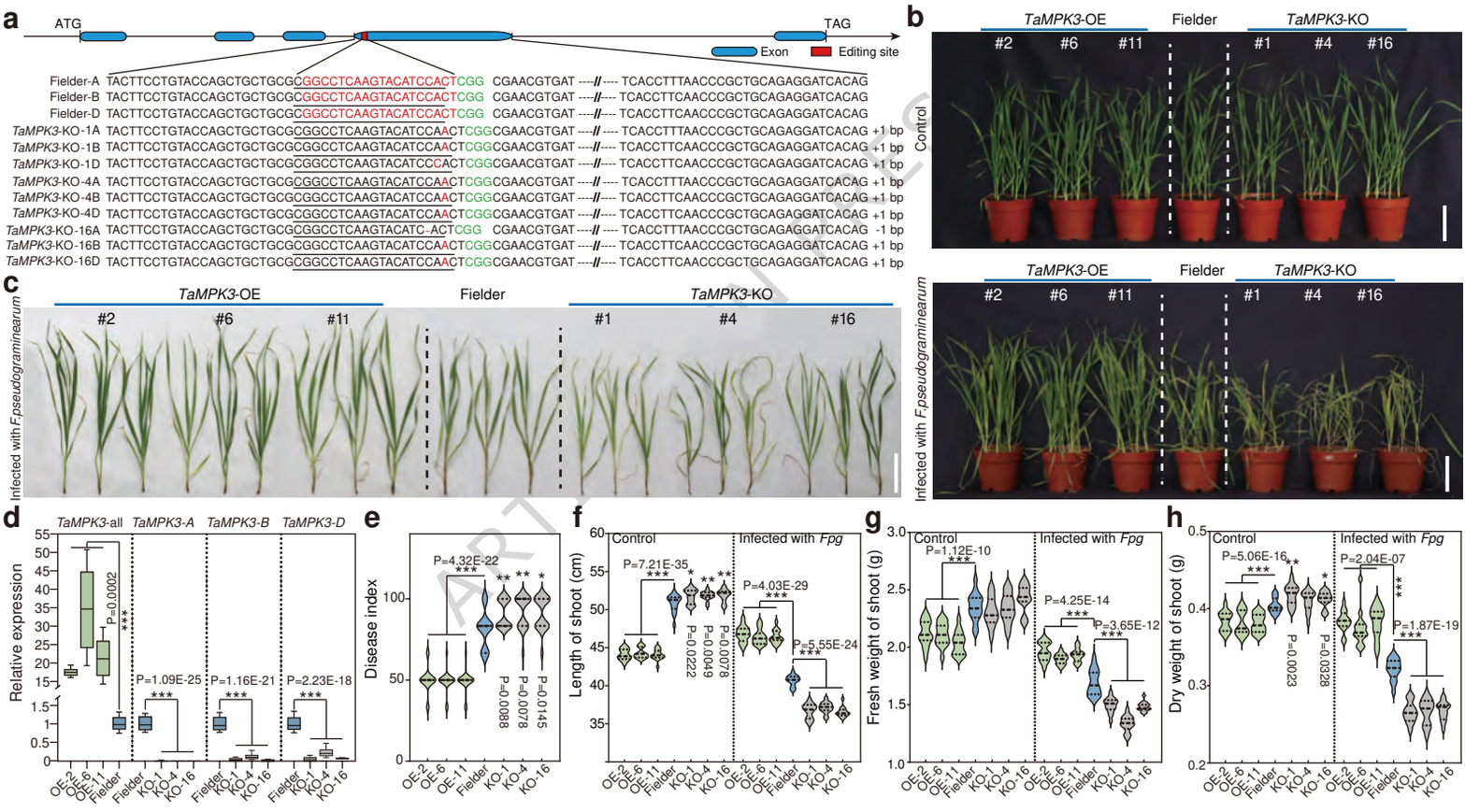
a
ATG
TAG
Exon
Editing site
Fielder-A TACTTCCTGTACCAGCTGCTGCGCGGCCTCAAGTACATCCACTCGG CGAACGTGAT ----//---- TCACCTTTAACCCGCTGCAGAGGATCACAG
Fielder-B TACTTCCTGTACCAGCTGCTGCGCGGCCTCAAGTACATCCACTCGG CGAACGTGAT ----//---- TCACCTTCAACCCGCTGCAGAGGATCACAG
Fielder-D TACTTCCTGTACCAGCTGCTGCGCGGCCTCAAGTACATCCACTCGG CGAACGTGAT ----//---- TCACCTTCAACCCGCTGCAGAGGATCACAG
TaMPK3-KO-1A TACTTCCTGTACCAGCTGCTGCGCGGCCTCAAGTACATCCAACTCGGCGAACGTGAT ----// ---- TCACCTTTAACCCGCTGCAGAGGATCACAG +1 bp
TaMPK3-KO-1B TACTTCCTGTACCAGCTGCTGCGCGGCCTCAAGTACATCCAACTCGGCGAACGTGAT ----//---- TCACCTTCAACCCGCTGCAGAGGATCACAG +1 bp
TaMPK3-KO-1D TACTTCCTGTACCAGCTGCTGCGCGGCCTCAAGTACATCCCACTCGGCGAACGTGAT ----//---- TCACCTTCAACCCGCTGCAGAGGATCACAG +1 bp
TaMPK3-KO-4A TACTTCCTGTACCAGCTGCTGCGCGGCCTCAAGTACATCCAACTCGGCGAACGTGAT ----// ---- TCACCTTTAACCCGCTGCAGAGGATCACAG +1 bp
TaMPK3-KO-4B TACTTCCTGTACCAGCTGCTGCGCGGCCTCAAGTACATCCAACTCGGCGAACGTGAT ----//---- TCACCTTCAACCCGCTGCAGAGGATCACAG +1 bp
TaMPK3-KO-4D TACTTCCTGTACCAGCTGCTGCGCGGCCTCAAGTACATCCAACTCGGCGAACGTGAT ----//---- TCACCTTCAACCCGCTGCAGAGGATCACAG +1 bp
TaMPK3-KO-16A TACTTCCTGTACCAGCTGCTGCGCGGCCTCAAGTACATC-ACTCGG CGAACGTGAT ----// ---- TCACCTTTAACCCGCTGCAGAGGATCACAG -1 bp
TaMPK3-KO-16B TACTTCCTGTACCAGCTGCTGCGCGGCCTCAAGTACATCCAACTCGGCGAACGTGAT ----//---- TCACCTTCAACCCGCTGCAGAGGATCACAG +1 bp
TaMPK3-KO-16D TACTTCCTGTACCAGCTGCTGCGCGGCCTCAAGTACATCCAACTCGGCGAACGTGAT ----//---- TCACCTTCAACCCGCTGCAGAGGATCACAG +1 bp
b
TaMPK3-OE
Fielder
TaMPK3-KO
#2
#6
#11
#1
#4
#16
Control
Infected with F.pseudograminearum
c
TaMPK3-OE
Fielder
TaMPK3-KO
#2
#6
#11
#1
#4
#16
Infected with F.pseudograminearum
d
TaMPK3-all
TaMPK3-A
TaMPK3-B
TaMPK3-D
Relative expression
P=0.0002
P=1.09E-25
P=1.16E-21
P=2.23E-18
OE-2
OE-6
OE-11
Fielder
KO-1
KO-4
KO-16
e
Disease index
P=4.32E-22
P=0.0088
P=0.0078
P=0.0145
f
Control
Infected with Fpg
Length of shoot (cm)
P=7.21E-35
P=0.0222
P=0.0049
P=0.0078
P=4.03E-29
P=5.55E-24
g
Control
Infected with Fpg
Fresh weight of shoot (g)
P=1.12E-10
P=4.25E-14
P=3.65E-12
h
Control
Infected with Fpg
Dry weight of shoot (g)
P=5.06E-16
P=0.0023
P=0.0328
P=2.04E-07
P=1.87E-19

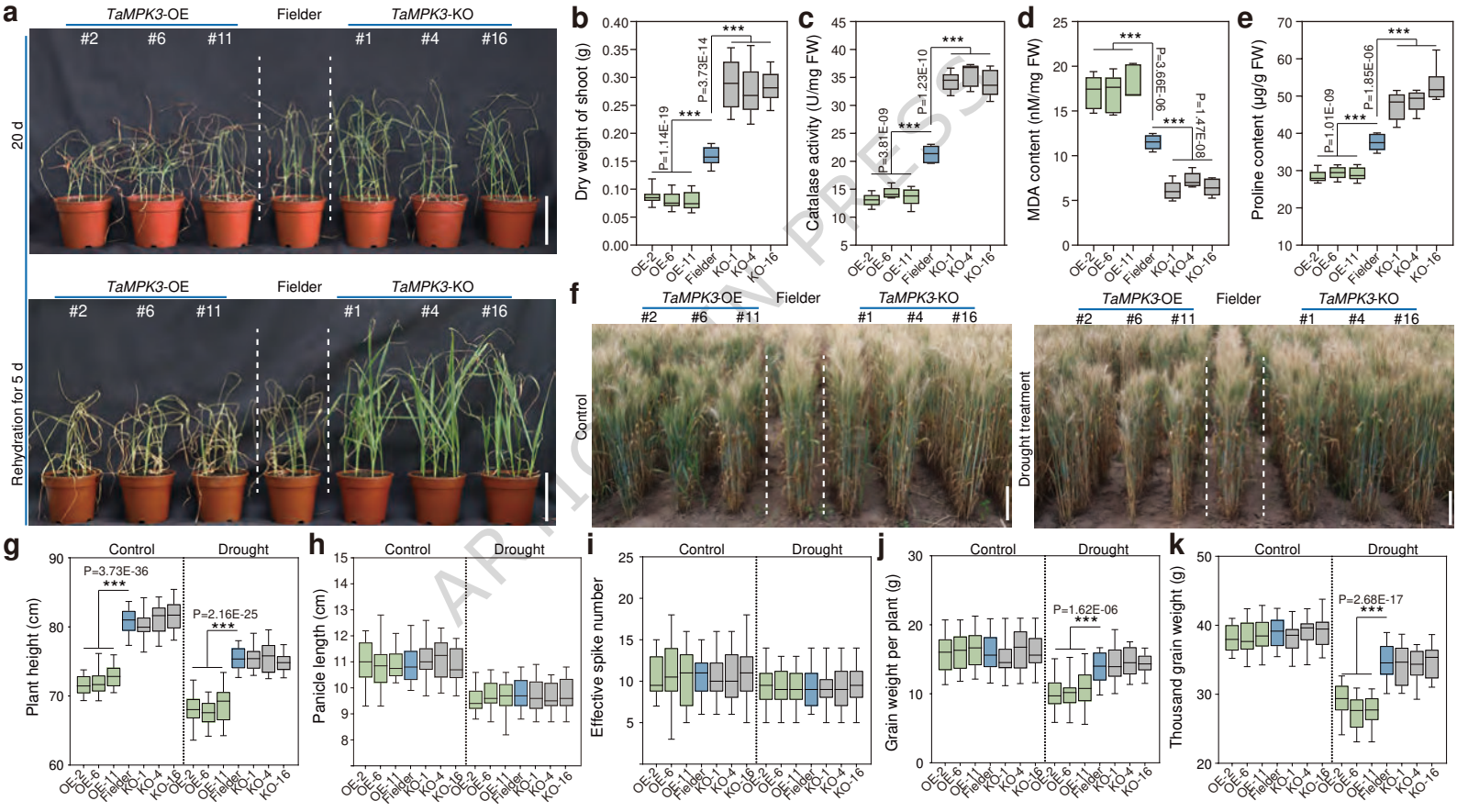
a
TaMPK3-OE
Fielder
TaMPK3-KO
#2
#6
#11
#1
#4
#16
20 d
Rehydration for 5 d
b
Dry weight of shoot (g)
P=1.14E-19
P=3.73E-14
c
Catalase activity (U/mg FW)
P=3.81E-09
P=1.23E-10
d
MDA content (nM/mg FW)
P=3.66E-06
P=1.47E-08
e
Proline content (μg/g FW)
P=1.01E-09
P=1.85E-06
OE-2
OE-6
OE-11
Fielder
KO-1
KO-4
KO-16
f
Control
Drought treatment
g
Plant height (cm)
P=3.73E-36
P=2.16E-25
h
Panicle length (cm)
i
Effective spike number
j
Grain weight per plant (g)
P=1.62E-06
k
Thousand grain weight (g)
P=2.68E-17
Control
Drought

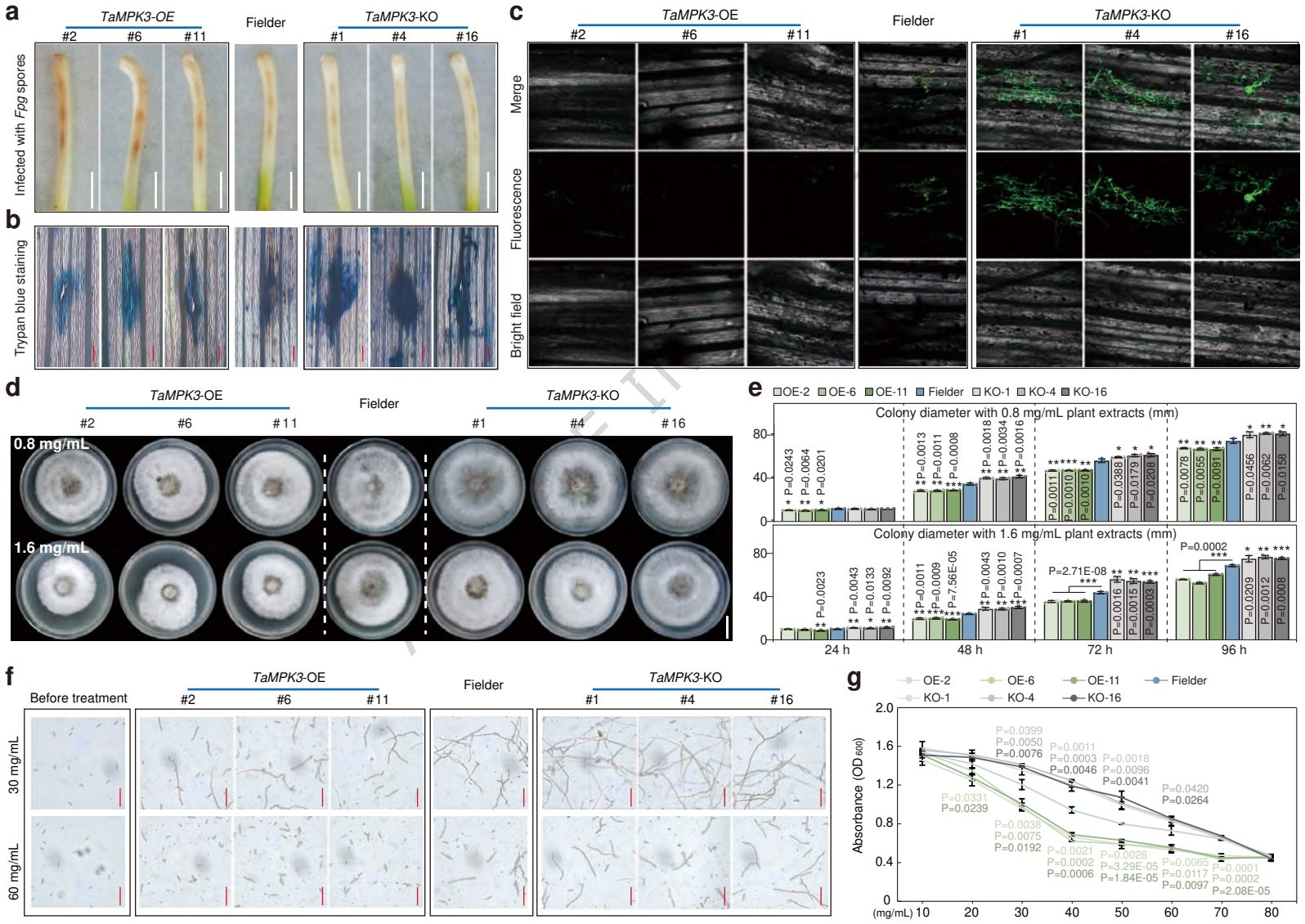
a
TaMPK3-OE
#2
#6
#11
Fielder
TaMPK3-KO
#1
#4
#16
Infected with Fpg spores
b
Trypan blue staining
c
TaMPK3-OE
#2
#6
#11
Fielder
TaMPK3-KO
#1
#4
#16
Merge
Fluorescence
Bright field
d
TaMPK3-OE
#2
#6
#11
Fielder
TaMPK3-KO
#1
#4
#16
0.8 mg/mL
1.6 mg/mL
e
OE-2
OE-6
OE-11
Fielder
KO-1
KO-4
KO-16
Colony diameter with 0.8 mg/mL plant extracts (mm)
Colony diameter with 1.6 mg/mL plant extracts (mm)
24 h
48 h
72 h
96 h
f
Before treatment
TaMPK3-OE
#2
#6
#11
Fielder
TaMPK3-KO
#1
#4
#16
30 mg/mL
60 mg/mL
g
OE-2
OE-6
OE-11
Fielder
KO-1
KO-4
KO-16
Absorbance (OD600)
(mg/mL)

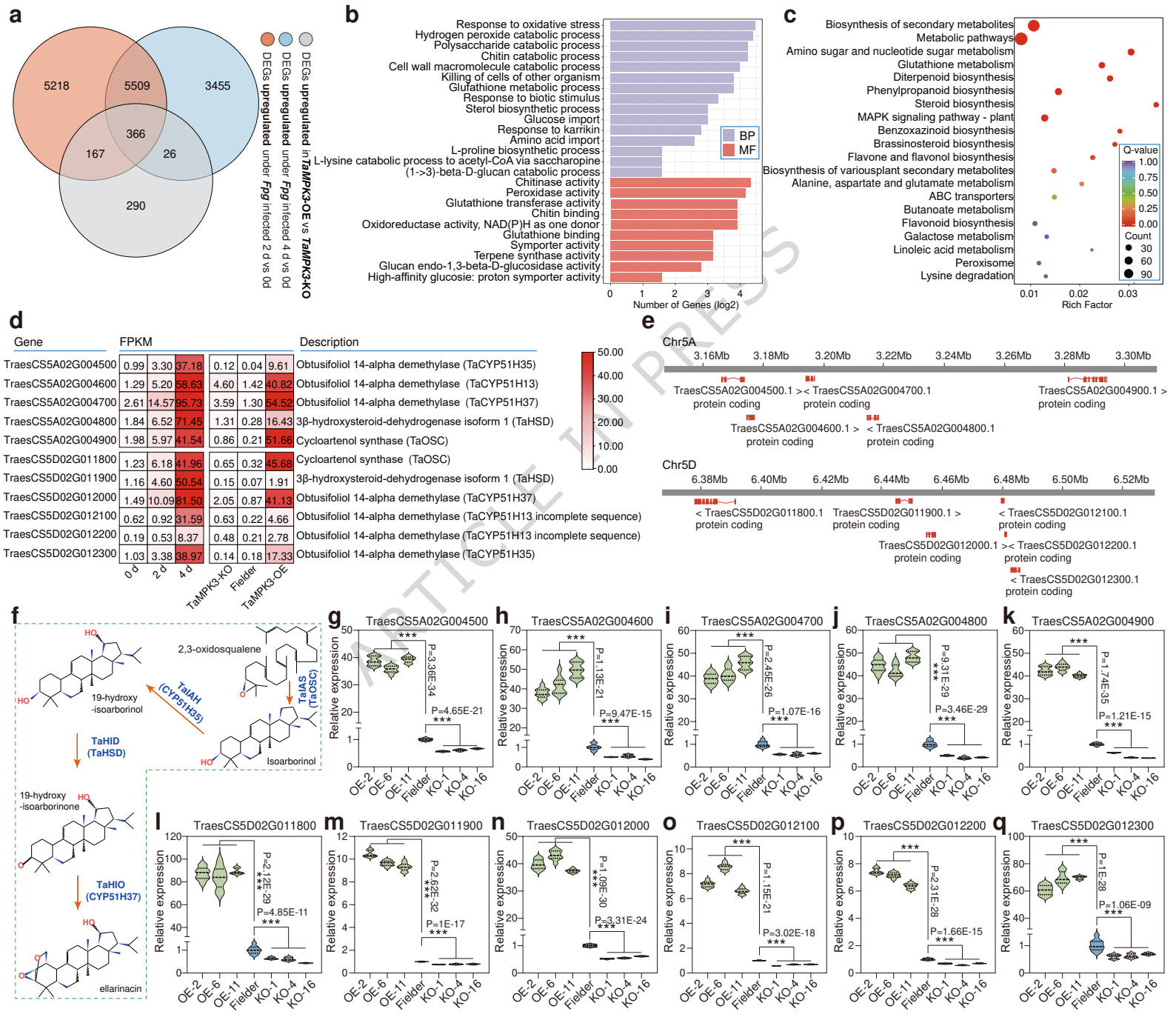

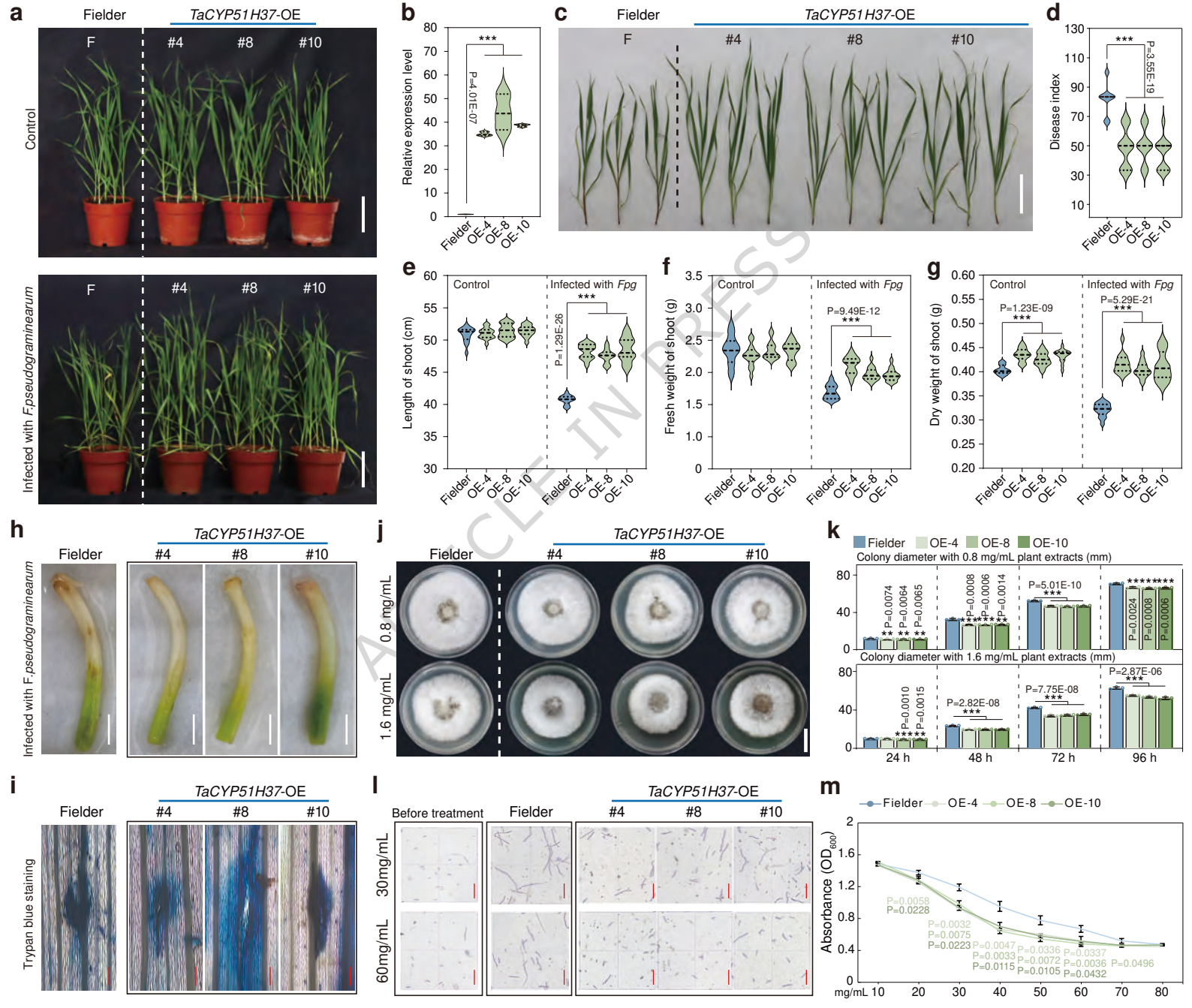
a
Fielder
TaCYP51H37-OE
F
#4
#8
#10
Control
Infected with F.pseudograminearum
b
Relative expression level
***
P=4.01E-07
Fielder
OE-4
OE-8
OE-10
c
Fielder
TaCYP51H37-OE
F
#4
#8
#10
d
Disease index
***
P=3.55E-19
e
Length of shoot (cm)
Control
Infected with Fpg
***
P=1.29E-26
f
Fresh weight of shoot (g)
Control
Infected with Fpg
***
P=9.49E-12
g
Dry weight of shoot (g)
Control
Infected with Fpg
P=1.23E-09
***
P=5.29E-21
h
Infected with F.pseudograminearum
Fielder
TaCYP51H37-OE
#4
#8
#10
j
Fielder
TaCYP51H37-OE
#4
#8
#10
0.8 mg/mL
1.6 mg/mL
k
Fielder
OE-4
OE-8
OE-10
Colony diameter with 0.8 mg/mL plant extracts (mm)
P=0.0074
P=0.0064
P=0.0065
P=0.0008
P=0.0006
P=0.0014
P=5.01E-10
***
P=0.0024
P=0.0008
P=0.0006
Colony diameter with 1.6 mg/mL plant extracts (mm)
P=0.0010
P=0.0015
P=2.82E-08
***
P=7.75E-08
***
P=2.87E-06
***
24 h
48 h
72 h
96 h
i
Trypan blue staining
Fielder
TaCYP51H37-OE
#4
#8
#10
l
Before treatment
Fielder
TaCYP51H37-OE
#4
#8
#10
30mg/mL
60mg/mL
m
Fielder
OE-4
OE-8
OE-10
Absorbance (OD600)
mg/mL
P=0.0058
P=0.0228
P=0.0032
P=0.0075
P=0.0223
P=0.0047
P=0.0033
P=0.0115
P=0.0336
P=0.0072
P=0.0105
P=0.0337
P=0.0036
P=0.0432
P=0.0496

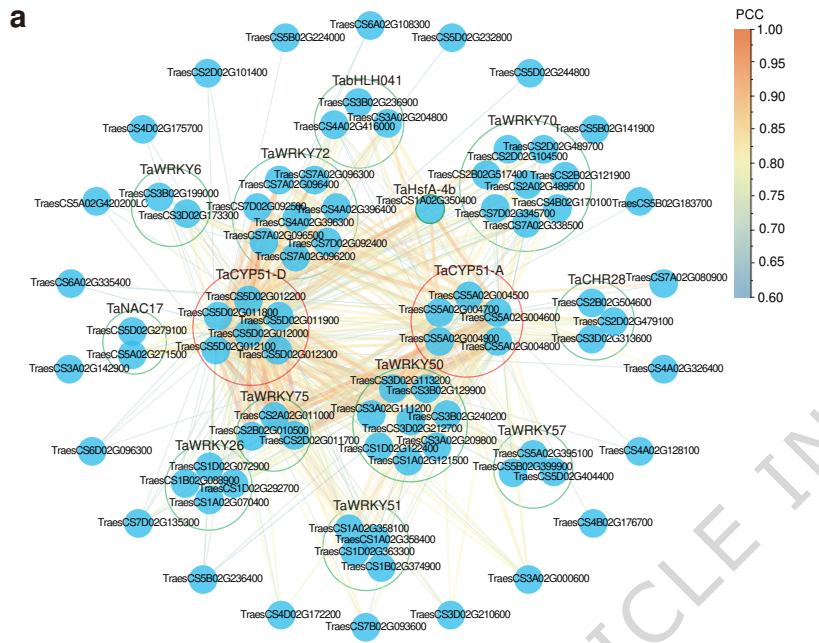
a
PCC
1.00
0.95
0.90
0.85
0.80
0.75
0.70
0.65
0.60
TaWRKY6
TaWRKY72
TabHLH041
TaWRKY70
TaHsfA-4b
TaCYP51-D
TaCYP51-A
TaCHR28
TaNAC17
TaWRKY50
TaWRKY75
TaWRKY57
TaWRKY26
TaWRKY51

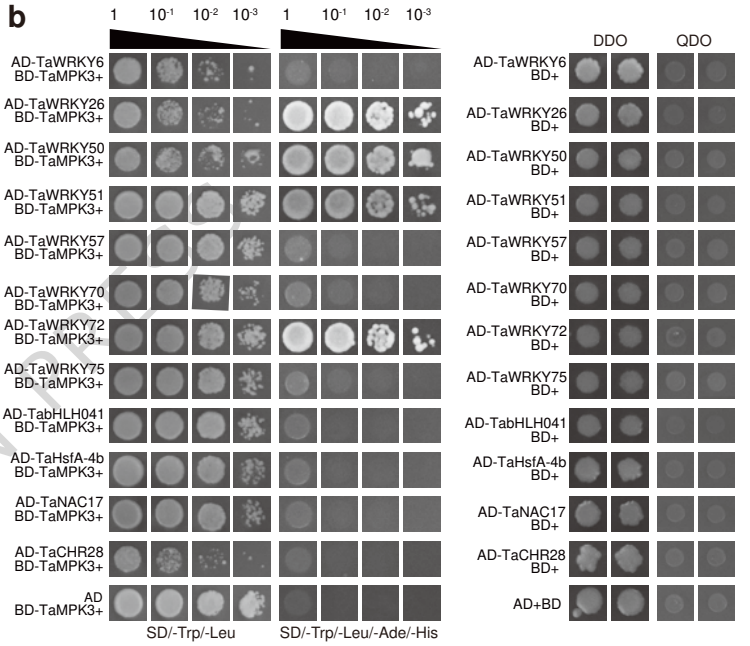
b
1
10-1
10-2
10-3
DDO
QDO
AD-TaWRKY6 BD-TaMPK3+
AD-TaWRKY26 BD-TaMPK3+
AD-TaWRKY50 BD-TaMPK3+
AD-TaWRKY51 BD-TaMPK3+
AD-TaWRKY57 BD-TaMPK3+
AD-TaWRKY70 BD-TaMPK3+
AD-TaWRKY72 BD-TaMPK3+
AD-TaWRKY75 BD-TaMPK3+
AD-TabHLH041 BD-TaMPK3+
AD-TaHsfA-4b BD-TaMPK3+
AD-TaNAC17 BD-TaMPK3+
AD-TaCHR28 BD-TaMPK3+
AD BD-TaMPK3+
AD-TaWRKY6 BD+
AD-TaWRKY26 BD+
AD-TaWRKY50 BD+
AD-TaWRKY51 BD+
AD-TaWRKY57 BD+
AD-TaWRKY70 BD+
AD-TaWRKY72 BD+
AD-TaWRKY75 BD+
AD-TabHLH041 BD+
AD-TaHsfA-4b BD+
AD-TaNAC17 BD+
AD-TaCHR28 BD+
AD+BD
SD/-Trp/-Leu
SD/-Trp/-Leu/-Ade/-His

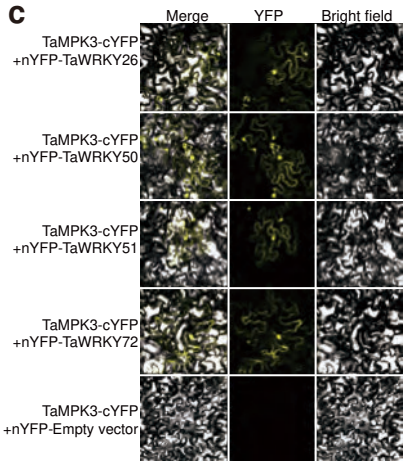
c
Merge
YFP
Bright field
TaMPK3-cYFP +nYFP-TaWRKY26
TaMPK3-cYFP +nYFP-TaWRKY50
TaMPK3-cYFP +nYFP-TaWRKY51
TaMPK3-cYFP +nYFP-TaWRKY72
TaMPK3-cYFP +nYFP-Empty vector

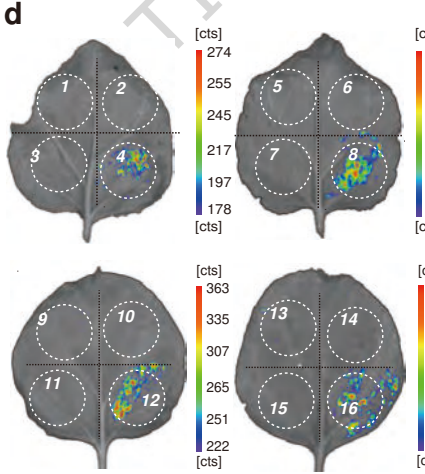
d
[cts]
274
255
245
217
197
178
1: nLUC+cLUC
2: nLUC+TaWRKY26-cLUC
3: TaMPK3-nLUC+cLUC
4: TaMPK3-nLUC+ TaWRKY26-cLUC
283
261
239
217
195
173
5: nLUC+cLUC
6: nLUC+TaWRKY50-cLUC
7: TaMPK3-nLUC+cLUC
8: TaMPK3-nLUC+ TaWRKY50-cLUC
363
335
307
265
251
222
9: nLUC+cLUC
10: nLUC+TaWRKY51-cLUC
11: TaMPK3-nLUC+cLUC
12: TaMPK3-nLUC+ TaWRKY51-cLUC
244
230
215
200
185
170
13: nLUC+cLUC
14: nLUC+TaWRKY72-cLUC
15: TaMPK3-nLUC+cLUC
16: TaMPK3-nLUC+ TaWRKY72-cLUC

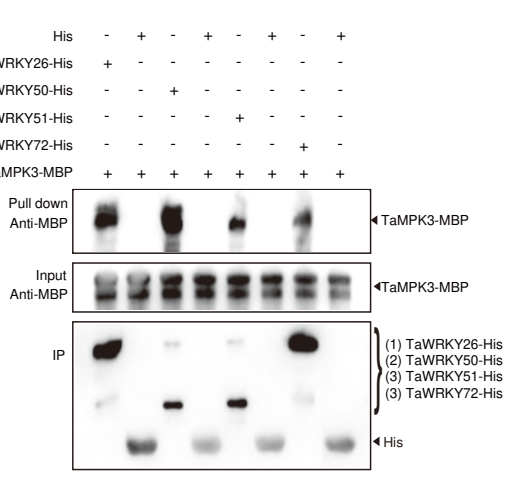
e
His
TaWRKY26-His
TaWRKY50-His
TaWRKY51-His
TaWRKY72-His
TaMPK3-MBP
Pull down Anti-MBP
Input Anti-MBP
IP
TaMPK3-MBP
(1) TaWRKY26-His
(2) TaWRKY50-His
(3) TaWRKY51-His
(3) TaWRKY72-His
His

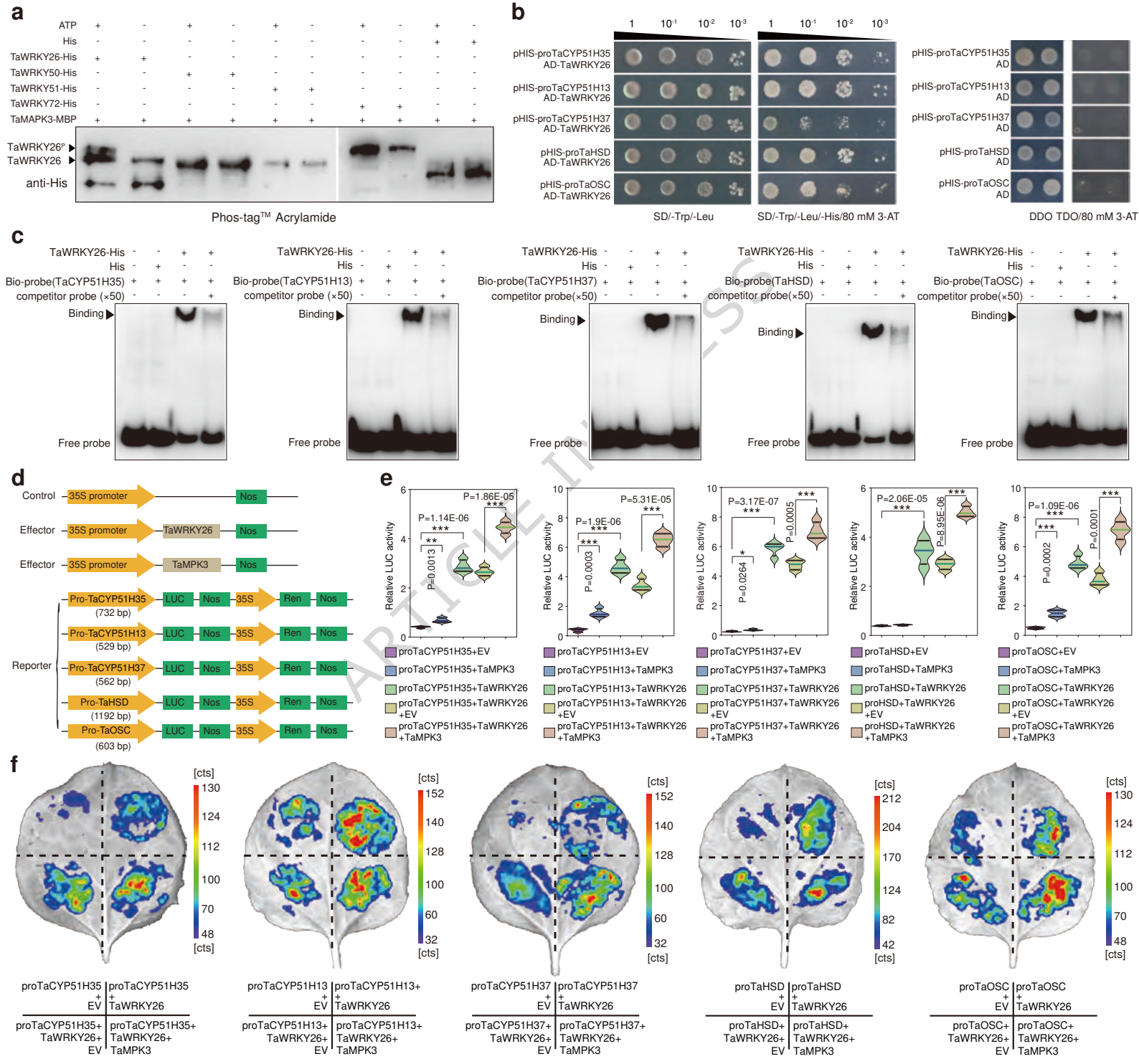
a
ATP
His
TaWRKY26-His
TaWRKY50-His
TaWRKY51-His
TaWRKY72-His
TaMAPK3-MBP
TaWRKY26P
TaWRKY26
anti-His
Phos-tag™ Acrylamide
b
1 10-1 10-2 10-3
pHIS-proTaCYP51H35 AD-TaWRKY26
pHIS-proTaCYP51H13 AD-TaWRKY26
pHIS-proTaCYP51H37 AD-TaWRKY26
pHIS-proTaHSD AD-TaWRKY26
pHIS-proTaOSC AD-TaWRKY26
SD/-Trp/-Leu
SD/-Trp/-Leu/-His/80 mM 3-AT
pHIS-proTaCYP51H35 AD
pHIS-proTaCYP51H13 AD
pHIS-proTaCYP51H37 AD
pHIS-proTaHSD AD
pHIS-proTaOSC AD
DDO TDO/80 mM 3-AT
c
TaWRKY26-His
His
Bio-probe(TaCYP51H35)
competitor probe (×50)
Binding
Free probe
Bio-probe(TaCYP51H13)
Bio-probe(TaCYP51H37)
Bio-probe(TaHSD)
Bio-probe(TaOSC)
d
Control
Effector
35S promoter
Nos
TaWRKY26
TaMAPK3
Reporter
Pro-TaCYP51H35
(732 bp)
Pro-TaCYP51H13
(529 bp)
Pro-TaCYP51H37
(562 bp)
Pro-TaHSD
(1192 bp)
Pro-TaOSC
(603 bp)
LUC
35S
Ren
e
Relative LUC activity
P=1.14E-06
P=0.0013
P=1.86E-05
P=1.9E-06
P=0.0003
P=5.31E-05
P=3.17E-07
P=0.0264
P=0.0005
P=2.06E-05
P=8.95E-06
P=1.09E-06
P=0.0002
P=0.0001
proTaCYP51H35+EV
proTaCYP51H35+TaMPK3
proTaCYP51H35+TaWRKY26
proTaCYP51H35+TaWRKY26 +EV
proTaCYP51H35+TaWRKY26 +TaMPK3
proTaCYP51H13+EV
proTaCYP51H13+TaMPK3
proTaCYP51H13+TaWRKY26
proTaCYP51H13+TaWRKY26 +EV
proTaCYP51H13+TaWRKY26 +TaMPK3
proTaCYP51H37+EV
proTaCYP51H37+TaMPK3
proTaCYP51H37+TaWRKY26
proTaCYP51H37+TaWRKY26 +EV
proTaCYP51H37+TaWRKY26 +TaMPK3
proTaHSD+EV
proTaHSD+TaMPK3
proTaHSD+TaWRKY26
proHSD+TaWRKY26 +EV
proHSD+TaWRKY26 +TaMPK3
proTaOSC+EV
proTaOSC+TaMPK3
proTaOSC+TaWRKY26
proTaOSC+TaWRKY26 +EV
proTaOSC+TaWRKY26 +TaMPK3
f
[cts]
proTaCYP51H35 + EV
proTaCYP51H35 + TaWRKY26
proTaCYP51H35+ TaWRKY26+ EV
proTaCYP51H35+ TaWRKY26+ TaMPK3
proTaCYP51H13 + EV
proTaCYP51H13 + TaWRKY26
proTaCYP51H13+ TaWRKY26+ EV
proTaCYP51H13+ TaWRKY26+ TaMPK3
proTaCYP51H37 + EV
proTaCYP51H37 + TaWRKY26
proTaCYP51H37+ TaWRKY26+ EV
proTaCYP51H37+ TaWRKY26+ TaMPK3
proTaHSD + EV
proTaHSD + TaWRKY26
proTaHSD+ TaWRKY26+ EV
proTaHSD+ TaWRKY26+ TaMPK3
proTaOSC + EV
proTaOSC + TaWRKY26
proTaOSC+ TaWRKY26+ EV
proTaOSC+ TaWRKY26+ TaMPK3

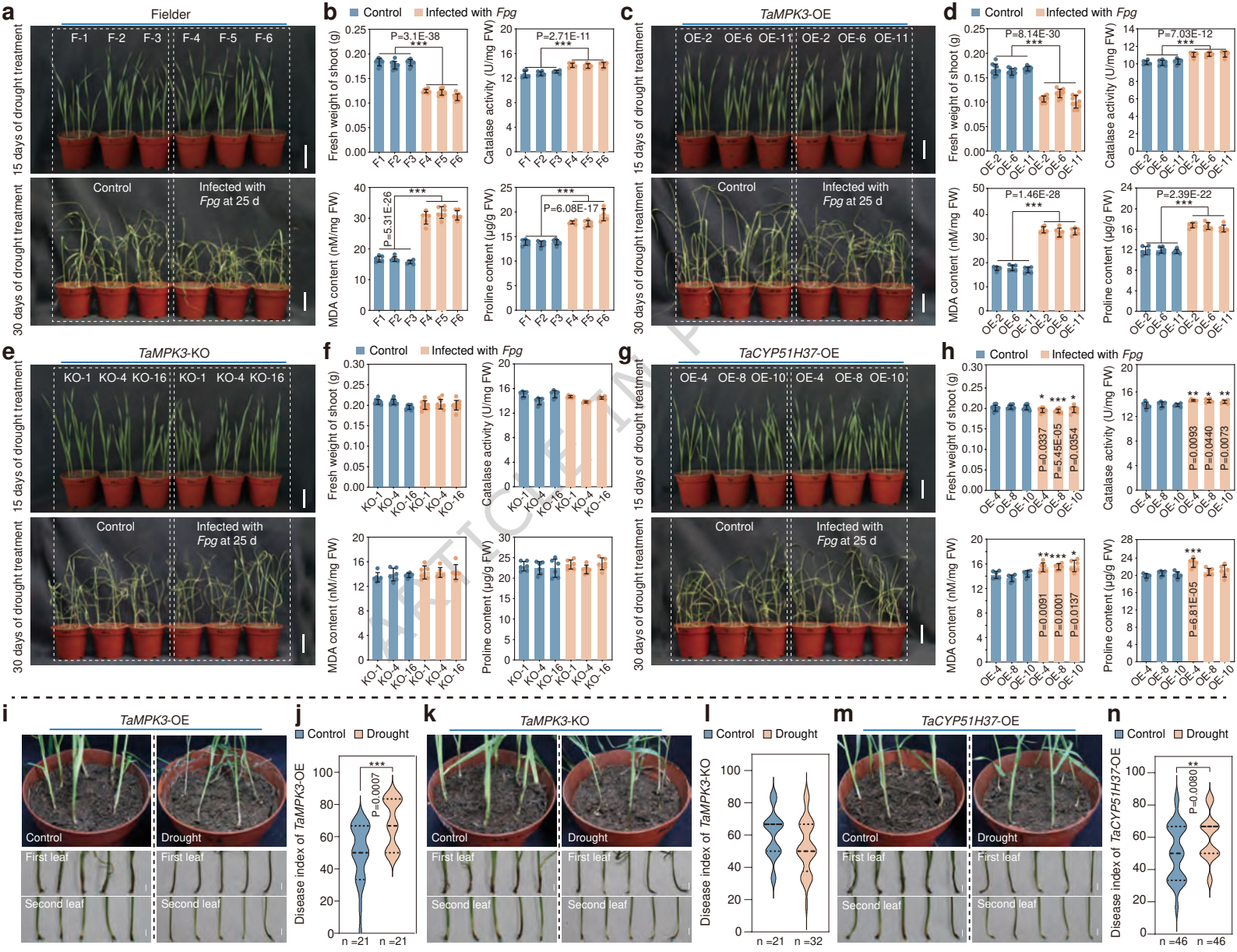
a
Fielder
F-1 F-2 F-3 F-4 F-5 F-6
15 days of drought treatment
30 days of drought treatment
Control
Infected with Fpg at 25 d
b
Control
Infected with Fpg
Fresh weight of shoot (g)
P=3.1E-38
***
Catalase activity (U/mg FW)
P=2.71E-11
***
MDA content (nM/mg FW)
P=5.31E-26
***
Proline content (μg/g FW)
P=6.08E-17
***
F1 F2 F3 F4 F5 F6
c
TaMPK3-OE
OE-2 OE-6 OE-11 OE-2 OE-6 OE-11
15 days of drought treatment
30 days of drought treatment
Control
Infected with Fpg at 25 d
d
Control
Infected with Fpg
Fresh weight of shoot (g)
P=8.14E-30
***
Catalase activity (U/mg FW)
P=7.03E-12
***
MDA content (nM/mg FW)
P=1.46E-28
***
Proline content (μg/g FW)
P=2.39E-22
***
OE-2 OE-6 OE-11 OE-2 OE-6 OE-11
e
TaMPK3-KO
KO-1 KO-4 KO-16 KO-1 KO-4 KO-16
15 days of drought treatment
30 days of drought treatment
Control
Infected with Fpg at 25 d
f
Control
Infected with Fpg
Fresh weight of shoot (g)
Catalase activity (U/mg FW)
MDA content (nM/mg FW)
Proline content (μg/g FW)
KO-1 KO-4 KO-16 KO-1 KO-4 KO-16
g
TaCYP51H37-OE
OE-4 OE-8 OE-10 OE-4 OE-8 OE-10
15 days of drought treatment
30 days of drought treatment
Control
Infected with Fpg at 25 d
h
Control
Infected with Fpg
Fresh weight of shoot (g)
P=0.0337
P=5.45E-05
P=0.0354
Catalase activity (U/mg FW)
P=0.0093
P=0.0440
P=0.0073
MDA content (nM/mg FW)
P=0.0091
P=0.0001
P=0.0137
Proline content (μg/g FW)
P=6.81E-05
OE-4 OE-8 OE-10 OE-4 OE-8 OE-10
i
TaMPK3-OE
Control
Drought
First leaf
Second leaf
j
Control
Drought
Disease index of TaMPK3-OE
P=0.0007
***
n =21 n =21
k
TaMPK3-KO
Control
Drought
First leaf
Second leaf
l
Control
Drought
Disease index of TaMPK3-KO
n =21 n =32
m
TaCYP51H37-OE
Control
Drought
First leaf
Second leaf
n
Control
Drought
Disease index of TaCYP51H37-OE
P=0.0080
**
n =46 n =46